SIAM J. Applied Dynamical Systems
Vol. 17, No. 1, pp. 859–908

Le Canard de Painlevé*

K. Uldall Kristiansen† and S. J. Hogan‡

Abstract. We consider the problem of a slender rod slipping along a rough surface. Painlevé [*C. R. Séances Acad. Sci.*, 121 (1895), pp. 112–115; *C. R. Séances Acad. Sci.*, 141 (1905), pp. 401–405; *C. R. Séances Acad. Sci.*, 141 (1905), pp. 546–552] showed that the governing rigid body equations for this problem can exhibit multiple solutions (the *indeterminate* case) or no solutions at all (the *inconsistent* case), provided the coefficient of friction μ exceeds a certain critical value μ_P. Subsequently Génot and Brogliato [*Eur. J. Mech. A Solids*, 18 (1999), pp. 653–677] proved that, from a consistent state, the rod cannot reach an inconsistent state through slipping. Instead the rod will either stop slipping and stick or it will lift off from the surface. Between these two cases is a special solution for $\mu > \mu_C > \mu_P$, where μ_C is a new critical value of the coefficient of friction. Physically, the special solution corresponds to the rod slipping until it reaches a singular "0/0" point P. Even though the rigid body equations cannot describe what happens to the rod beyond the singular point P, it is possible to extend the special solution into the region of indeterminacy. This extended solution is very reminiscent of a *canard* [E. Benoît et al., *Collect. Math.*, 31-32 (1981), pp. 37–119]. To overcome the inadequacy of the rigid body equations beyond P, the rigid body assumption is relaxed in the neighborhood of the point of contact of the rod with the rough surface. Physically this corresponds to assuming a small compliance there. It is natural to ask what happens to both the point P and the special solution under this regularization, in the limit of vanishing compliance. In this paper, we prove the existence of a canard orbit in a reduced four-dimensional slow-fast phase space, connecting a two-dimensional focus-type slow manifold with the stable manifold of a two-dimensional saddle-type slow manifold. The proof combines several methods from local dynamical system theory, including blowup. The analysis is not standard, since we only gain ellipticity rather than hyperbolicity with our initial blowup.

Key words. Painlevé paradox, impact without collision, compliance, regularization

AMS subject classifications. 70E18, 34E15, 34E17

DOI. 10.1137/17M1122256

1. Introduction.

In a series of classical papers, Painlevé [45, 46, 47] showed that the governing equations for a slender rod slipping along a rough surface (see Figure 1) can exhibit multiple solutions (the *indeterminate* case) or no solutions at all (the *inconsistent* case), provided the coefficient of friction μ exceeds a certain critical value μ_P. In the intervening years, a large number of authors [2, 4, 6, 50] have considered different aspects of these *Painlevé paradoxes*, which have been shown to occur in many important engineering systems [36, 37, 39, 43, 44, 56, 57, 59].

*Received by the editors March 23, 2017; accepted for publication (in revised form) by J. Sieber November 21, 2017; published electronically March 27, 2018.
http://www.siam.org/journals/siads/17-1/M112225.html
†Department of Applied Mathematics and Computer Science, Technical University of Denmark, 2800 Kgs. Lyngby, Denmark (krkri@dtu.dk).
‡Department of Engineering Mathematics, University of Bristol, Bristol BS8 1UB, UK (s.j.hogan@bristol.ac.uk).

The theoretical study of Painlevé paradoxes received a great boost with the work by Génot and Brogliato [19], who discovered a new critical value of the coefficient of friction $\mu_C > \mu_P$. They proved that, from a consistent state, the rod cannot reach an inconsistent state through slipping. Instead, the rod will either stop slipping and stick or it will lift off from the surface. For $\mu > \mu_C$, these cases are separated by a special solution where the rod slips until it reaches a singular point P corresponding to a "0/0"-singularity in the equations of motion. Beyond P, the rigid body equations are unable to predict what happens. Nevertheless, it is possible to extend the special solution beyond the singular point P into the region of indeterminacy. Therefore this extended solution is very reminiscent of a *canard* [1] that occurs at folded equilibria in $(2+1)$-slow-fast systems[1] [52, 55] and in the two-fold of piecewise smooth (PWS) systems [9, 25, 26, 27].

Ever since the time of Painlevé, there have been attempts to resolve the paradoxes by including more physics into the rigid body formalism. Lecornu [35] proposed that a jump in vertical velocity would allow for an escape from an inconsistent, horizontal velocity, state. This jump has been called *impact without collision* (IWC) [19], *tangential impact* [22], or *dynamic jamming* [44]. During (the necessarily instantaneous) IWC, the governing equations of motion must be expressed in terms of the normal impulse, rather than time [8, 24]. But this approach can produce contradictions, such as an apparent energy gain in the presence of friction [3, 51].

Another possible way to resolve the Painlevé paradox is to relax the rigid body assumption in the neighborhood of the contact point. Physically this corresponds to assuming a small compliance, usually modeled as a spring, with large stiffness and (possibly) damping. Dupont and Yamajako [14] appear to be the first to show that the classical Painlevé problem with compliance could then be written as a slow-fast system. They showed that the fast subsystem is unstable in the Painlevé paradox. Song et al. [49] extended this work and established conditions under which the fast solution can be stabilized. Zhao et al. [58] considered the example in Figure 1 and regularized the equations by assuming a compliance that consisted of an *undamped* spring. They gave estimates for the time taken in the resulting stages of the dynamics. Neimark and Smirnova [40, 41] considered a different type of regularization in which the normal and tangential reactions take (different) finite times to adjust. Their results showed a strong dependence on the ratio of these times. More recently, the current authors presented [21] the first *rigorous* analysis of compliant IWC in both the inconsistent and indeterminate cases and gave explicit asymptotic expressions in the limiting cases of small and large damping. For the indeterminate case, we presented a formula for conditions that separate compliant IWC and lift-off.

In this paper, we consider the dynamics of the special solution (canard) around P in the presence of compliance. This will give rise to a (2+2)-slow-fast system with small parameter ε being the inverse square root of the stiffness associated with the compliance. Slow-fast systems receive an enormous amount of attention, since they occur naturally in many biological and engineering systems. As the recent book by Kuehn [31] and other works have made clear, a major boost to the subject came about following the seminal work of Fenichel [15, 16, 17] and the development of geometric singular perturbation theory (GSPT) [23]. Fenichel theory and GSPT work away from critical points, such as folds and singularities (specifically any point

[1] An $(n+m)$-slow-fast system [31] is a dynamical system with n slow variables and m fast variables.

where hyperbolicity is lost). At such points, GSPT has to be extended. Such an extension was made possible by the pioneering work of Dumortier and Roussarie [11, 12, 13]. Their approach, known as blowup, was further developed by Krupa and Szmolyan [28, 29, 30] to a form where it became popular and widely applicable to many different and challenging problems.[2]

It is also possible to study canards using blowup. Originally discovered by Benoît et al. [1], these are solutions to singularly perturbed problems that initially follow a stable manifold, then pass through a critical point, before following an unstable manifold for a nonvanishing period of time. Their study was significantly aided by the development of blowup, where the critical point had, until then, proved a barrier to the use of GSPT. Canards are important since they are crucial to the so-called canard explosion [5, 30], in which limit cycles are transformed, under parameter variation, into relaxation oscillations. The change happens over an exponentially small parameter range.[3]

We will apply blowup to the compliant (2+2)-slow-fast system and rigorously show the existence of a canard that connects, in the four-dimensional phase space, a two-dimensional (2D) attracting Fenichel slow manifold of focus-type with the stable manifold of a 2D saddle-type slow manifold (Theorem 6). The singular point P of the rigid body system becomes a line of Bogdanov–Takens (BT) points [48] of the layer problem associated with the regularization with a nilpotent 2×2 Jordan block. The mathematical difficulties in proving Theorem 6 are as follows. In the scaling chart associated with the blowup, we obtain the following equation:

$$\tilde{y}'''(\theta_2) = \theta_2 \tilde{y}'(\theta_2) + (1-\xi)\tilde{y}(\theta_2), \quad \theta_2 \in \mathbb{R}, \tag{1}$$

for $\xi \in (0,1)$. The third order linear ODE (1) appears to have been first considered by Langer [33, 34], as an example of an ODE in which the characteristic equation can have three coincident roots. See also [53, 54]. We will therefore refer to this equation as *Langer*'s equation[4] henceforth. Langer's equation also appears in [42], and so the Painlevé paradox would seem to be its first physically important application.

We will show (Lemma 13 in section 4.4) that Langer's equation has a distinguished solution

$$\mathrm{La}_\xi(\theta_2) = \int_0^\infty e^{-\tau^3/3+\theta_2\tau}\tau^{-\xi}d\tau,$$

which spans all solutions that are nonoscillatory for $\theta_2 \to -\infty$. All other solutions, spanned by special functions $\mathrm{Lb}_\xi(\theta_2)$, $\mathrm{Lc}_\xi(\theta_2)$, introduced in Lemma 13, are oscillatory as $\theta_2 \to -\infty$. Therefore, as a consequence, we only gain ellipticity (rather than hyperbolicity) of the focus-type slow manifold of the blowup of P (upon desingularization). So we apply normal form transformations—to eliminate fast oscillations—that will subsequently allow for an additional application of a (polar) blowup transformation. We gain hyperbolicity by this second transformation and are therefore able to extend Fenichel's slow manifold as a center-like manifold

[2] The present authors have successfully applied GSPT [25, 26, 27] to PWS problems [10], where the underlying vector fields have jumps or discontinuities that are then regularized.

[3] Canards are known to occur in PWS systems and their fate under regularization has been studied [9, 25, 26, 27].

[4] We are aware of a different *Langer's equation* in the theory of spinodal decomposition [32]. However this other equation postdates (1).

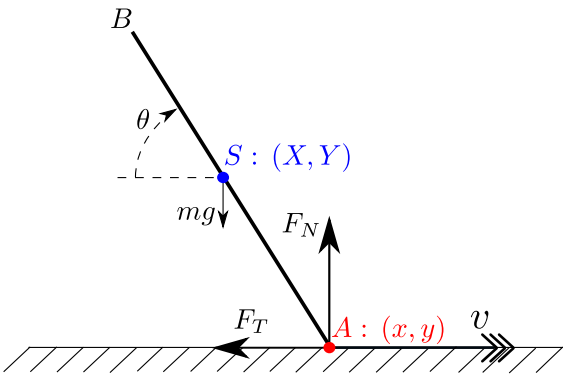

Figure 1. *The classical Painlevé problem: g is the acceleration due to gravity; the rod has mass m, length $2l$, the moment of inertia of the rod about its center of mass S is given by I, and its center of mass coincides with its center of gravity. The point S has coordinates (X, Y) relative to an inertial frame of reference (x, y) fixed in the rough surface. The rod makes an angle θ with respect to the horizontal, with θ increasing in a clockwise direction. At A, the rod experiences a contact force (F_T, F_N), which opposes the motion.*

up close to the point P (see Proposition 23 in Appendix B). But interestingly, this manifold does not extend all the way to the scaling chart. There is a gap which we can only cover by estimation of the forward flow. This brings us up close to the distinguished nonoscillatory solutions in the scaling chart for $0 < \varepsilon \ll 1$. We then complete our proof by using properties of $\mathrm{La}_\xi(\theta_2)$ for $\theta_2 \to \infty$.

The paper is organized as follows. In section 2, we introduce the classical Painlevé problem, outline some of the results due to Génot and Brogliato [19], show that $\mu_C = \frac{2}{\sqrt{3}}\mu_P$ for a large class of rigid bodies, introduce compliance, and, in (30), present our (2+2)-slow-fast system. In section 3, we summarize our main result, Theorem 6. The rest of the paper is devoted to the mathematical proof of Theorem 6, using blowup [28, 29, 30]. Section 4 sets up the initial blowup. The exit chart is considered in section 4.4, the scaling chart in section 4.5, and the entry chart in section 4.6. Each of sections 4.4 to 4.6 contains a number of technical propositions whose details are confined to the appendices. We discuss our results and outline our conclusions in section 5.

2. The classical Painlevé problem.

The governing equations[5] of the rigid rod AB of length $2l$ that slips on a rough horizontal surface, as shown in Figure 1, are given by

$$\begin{aligned} m\ddot{X} &= -F_T, \\ m\ddot{Y} &= -mg + F_N, \\ I\ddot{\theta} &= -l(\cos\theta F_N - \sin\theta F_T). \end{aligned} \tag{2}$$

[5]Painlevé [45] originally studied a planar box sliding down an inclined plane. Nevertheless, as noted in [6, p. 539], the problem most closely associated with Painlevé is the one in Figure 1. We will therefore also refer to this as the *classical Painlevé problem*.

From geometry

$$x = X + l\cos\theta, \tag{3}$$
$$y = Y - l\sin\theta.$$

We now define dimensionless variables and parameter α as follows:

$$l(\tilde{X},\tilde{Y}) = (X,Y), \quad l(\tilde{x},\tilde{y}) = (x,y), \quad mg(\tilde{F}_T,\tilde{F}_N) = (F_T,F_N), \quad \tilde{t} = \omega t, \quad \alpha = \frac{ml^2}{I},$$

where $\omega^2 = \frac{g}{l}$. For a uniform rod, $I = \frac{1}{3}ml^2$, and so $\alpha = 3$ in this case.

So for general α, by combining (2) and (3) and writing everything in terms of the dimensionless variables, and then dropping the tildes, we find

$$\begin{aligned}
\ddot{x} &= -\dot{\theta}^2\cos\theta + \alpha\sin\theta\cos\theta F_N - (1+\alpha\sin^2\theta)F_T, \\
\ddot{y} &= -1 + \dot{\theta}^2\sin\theta + (1+\alpha\cos^2\theta)F_N - \alpha\sin\theta\cos\theta F_T, \\
\ddot{\theta} &= -\alpha(\cos\theta F_N - \sin\theta F_T).
\end{aligned} \tag{4}$$

We assume Coulomb friction between the rod and the surface. So, when $\dot{x} = v \neq 0$, we set

$$F_T = \mu\,\mathrm{sign}(\dot{x})F_N, \tag{5}$$

where μ is the coefficient of friction. We introduce $\phi = \dot{\theta}$, $w = \dot{y}$, $v = \dot{x}$ and substitute (5) into (4) to get

$$\begin{aligned}
\dot{x} &= v, \\
\dot{v} &= a(\theta,\phi) + q_{\pm}(\theta)F_N, \\
\dot{y} &= w, \\
\dot{w} &= b(\theta,\phi) + p_{\pm}(\theta)F_N, \\
\dot{\theta} &= \phi, \\
\dot{\phi} &= c_{\pm}(\theta)F_N,
\end{aligned} \tag{6}$$

where

$$\begin{aligned}
a(\theta,\phi) &= -\phi^2\cos\theta, \\
b(\theta,\phi) &= -1 + \phi^2\sin\theta, \\
q_{\pm}(\theta) &= \alpha\sin\theta\cos\theta \mp \mu(1+\alpha\sin^2\theta), \\
p_{\pm}(\theta) &= 1 + \alpha\cos^2\theta \mp \mu\alpha\sin\theta\cos\theta, \\
c_{\pm}(\theta) &= -\alpha(\cos\theta \mp \mu\sin\theta)
\end{aligned} \tag{7}$$

for the configuration in Figure 1. The suffix $\pm$ corresponds to $\dot{x} = v \gtrless 0$, respectively.

We will suppose that the rod is initially moving to the right at time $t = 0$:

$$\dot{x}(0) = v(0) = v_0 > 0.$$

Then if, at some later time $t = T$, $\dot{x}(T) = v(T) = 0$ and $\dot{v}$ for $v \gtrless 0$ both oppose the discontinuity set $v = 0$: $\dot{v} < 0$ for $v = 0^+$ and $\dot{v} > 0$ for $v = 0^-$, the required vector-field is obtained by Filippov's method [18]; see [21]. We call this dynamics *sticking*. Note that by (7) it follows that $q_+ < 0$ whenever $p_+ \approx 0$.

We now need to determine F_N, using either the constraint-based method, which leads to a Painlevé paradox, or the compliance-based method, which is used in this paper.

2.1. Constraint-based method. In order to maintain the constraint $y = 0$, at most one of F_N and y can be positive [21] and so F_N and y must satisfy

$$0 \leq F_N \perp y \geq 0. \tag{8}$$

Hence, from (6), if $\dot{w} = 0$, then

$$F_N = -\frac{b}{p_+}, \tag{9}$$

since $v > 0$. Then we have a reduced, decoupled system in the (θ, ϕ)-plane:

$$\begin{aligned} \dot{\theta} &= \phi, \\ \dot{\phi} &= -\frac{c_\pm(\theta) b(\theta, \phi)}{p_+(\theta)}, \end{aligned} \tag{10}$$

and the variables x and v satisfy

$$\begin{aligned} \dot{x} &= v, \\ \dot{v} &= a(\theta, \phi) - \frac{q_\pm(\theta) b(\theta, \phi))}{p_+(\theta)}, \end{aligned}$$

which can be directly integrated once θ and ϕ are known.

For the system in Figure 1, Painlevé paradoxes occur when $v > 0$ and $\theta \in (0, \frac{\pi}{2})$, provided $p_+(\theta) < 0$ [21]. From (7), it is straightforward to show that $p_+(\theta) < 0$ requires

$$\mu > \mu_P(\alpha) \equiv \frac{2}{\alpha}\sqrt{1+\alpha}. \tag{11}$$

Then a Painlevé paradox occurs for $\theta \in (\theta_1, \theta_2)$, where

$$\begin{aligned} \theta_1(\mu, \alpha) &= \arctan \frac{1}{2}\left(\mu\alpha - \sqrt{\mu^2\alpha^2 - 4(1+\alpha)}\right), \\ \theta_2(\mu, \alpha) &= \arctan \frac{1}{2}\left(\mu\alpha + \sqrt{\mu^2\alpha^2 - 4(1+\alpha)}\right). \end{aligned} \tag{12}$$

For a uniform rod, $\mu_P(3) = \frac{4}{3}$. The dynamics in the (θ, ϕ)-plane[6] are shown in Figure 2 for $\alpha = 3$ and $\mu = 1.4$. The region $\theta \in (\theta_1, \theta_2)$, where $p_+(\theta) < 0$ is colored green and purple. In the green region, $b < 0$ and hence F_N in (9) is negative. This is the *inconsistent*

[6] Génot and Brogliato [19] plot in Figure 2 the *unscaled* angular velocity $\omega\phi$ *vs.* θ, where $\omega = \sqrt{\frac{g}{l}}$, for the case $g = 9.8$ ms^{-2}, $l = 1$ m.

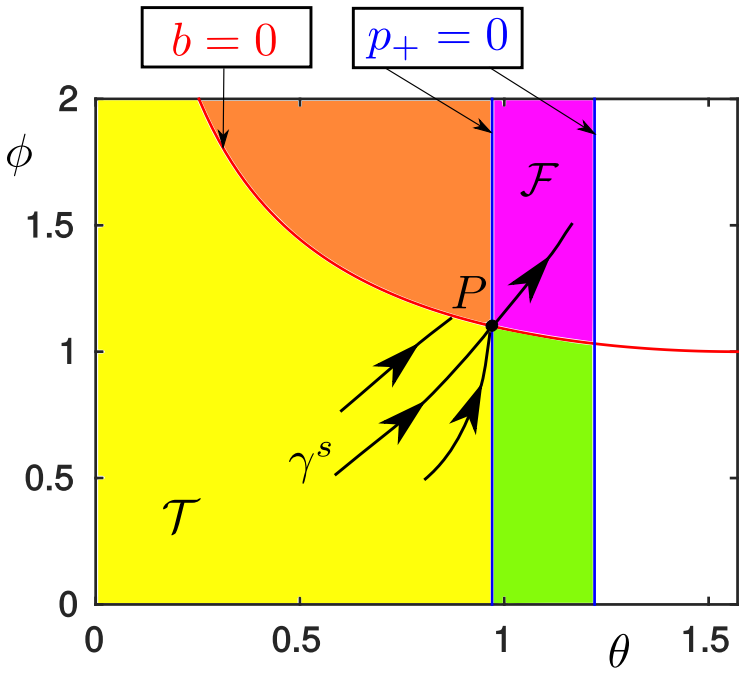

Figure 2. *The (θ, ϕ)-plane for the classical Painlevé problem of* Figure 1 *for $\alpha = 3$ and $\mu = 1.4$. The point P has coordinates $(\theta_1, \sqrt{\csc\theta_1})$, where θ_1 is given in (12). γ^s is defined in (17). In the purple region, $b > 0$, $p_+ < 0$, and the dynamics is indeterminate (nonunique). In the orange region, $b > 0$, $p_+ > 0$, and the rod lifts off the rough surface. In the yellow region, $b < 0$, $p_+ > 0$, and the rod moves (slips) along the surface. Finally, in the green region, $b < 0$, $p_+ < 0$, and the dynamics is inconsistent; there exists no positive value of F_N, even though the constraint $y = 0$ is satisfied, contrary to (8).*

(or *nonexistent*) mode of the Painlevé paradox. In the purple region, $b > 0$. From (6), b is the free acceleration of the end of the rod. Lift-off into $y > 0$ is therefore always possible within this region. At the same time F_N in (9) is positive. Hence, the purple region is the *indeterminate* (or *nonunique*) mode of the Painlevé paradox. The lines $p_+(\theta_{1,2}) = 0$ intersect $b(\theta, \phi) = 0$ at four points: $\phi^{\pm}_{1,2} = \pm\sqrt{\csc\theta_{1,2}}$. The point

$$P : (\theta, \phi) = (\theta_1, \sqrt{\csc\theta_1}) \tag{13}$$

is the most important [19]. Then we have the following.

Proposition 1. *Consider*

$$\begin{aligned} \mathcal{F} &= \{(\theta, \phi) | b(\theta, \phi) > 0,\ p_+(\theta) < 0\} \cap \mathcal{U}, \\ \mathcal{T} &= \{(\theta, \phi) | b(\theta, \phi) < 0,\ p_+(\theta) > 0\} \cap \mathcal{U}, \end{aligned} \tag{14}$$

where $\mathcal{U}$ is a small neighborhood of $P \in \{(\theta, \phi) | b(\theta, \phi) = 0,\ p_+(\theta) = 0\}$. Then the point P is a stable node of (10) within $\mathcal{U}$ with respect to a new time τ, satisfying

$$\frac{d\tau}{dt} = \frac{1}{p_+(\theta)}. \tag{15}$$

In particular, if

$$\mu > \mu_C(\alpha) = \frac{4}{\alpha}\sqrt{\frac{\alpha+1}{3}}, \tag{16}$$

then there exists a constant $c > 0$ sufficiently small and a smooth 1D invariant, strong stable manifold γ^s (of (23) below) within $\mathcal{T} \cup P \cup \mathcal{F}$,

$$\gamma^s : \quad \phi = m_{ss}(\theta) \equiv (1-\xi)^{-1} s\theta + \mathcal{O}(\theta^2), \quad \theta \in [\theta_1 - c, \theta_1 + c], \tag{17}$$

tangent to

$$(1-\xi, s)^T, \tag{18}$$

at P, where

$$\xi = \lambda_1^{-1}\lambda_2 \in (0,1), \tag{19}$$

$$s = -\lambda_1^{-1}(\phi_1^+)^2 > 0, \tag{20}$$

and $\lambda_{1,2} < 0$ are defined in (24) below. Every point in the subset

$$\mathcal{L} = \{(\theta,\phi) \in \mathcal{T} | \phi > m_{ss}(\theta)\} \tag{21}$$

leaves $\mathcal{T}$, under the forward flow of (10), through the boundary defined by $b(\theta,\phi) = 0$ while every point in the subset

$$\mathcal{S} = \{(\theta,\phi) \in \mathcal{T} | \phi < m_{ss}(\theta)\} \tag{22}$$

leaves $\mathcal{T}$ through P tangent to the vertical boundary $p(\theta,\phi) = 0$.

Proof. We include a simple proof of this proposition. In terms of τ we obtain from (10) and (15)

$$\begin{aligned} \frac{d\theta}{d\tau} &= p_+(\theta)\phi, \\ \frac{d\phi}{d\tau} &= -c_+(\theta)b(\theta,\phi). \end{aligned} \tag{23}$$

The point $P = (\theta_1, \phi_1^+)$ given in (13) is a fixed point of these equations. Linearization about P gives the Jacobian

$$\begin{pmatrix} p'_+(\theta_1)\phi_1^+ & 0 \\ -c_+(\theta_1)\partial_\theta b(\theta_1,\phi_1^+) & -c_+(\theta_1)\partial_\phi b(\theta_1,\phi_1^+) \end{pmatrix} = \begin{pmatrix} p'_+(\theta_1)\phi_1^+ & 0 \\ -(\phi_1^+)^2 & -2\tan(\theta_1)\phi_1^+ \end{pmatrix},$$

since $c_+(\theta_1) = \sec\theta_1$, which has eigenvalues

$$\lambda_1 = p'_+(\theta_1)\phi_1^+, \quad \lambda_2 = -c_+(\theta_1)\partial_\phi b(\theta_1,\phi_1^+) = -2\tan(\theta_1)\phi_1^+ \tag{24}$$

that are both negative in the range of θ_1 that contains the Painlevé paradox.

Simple algebraic manipulations show that

$$\xi = \lambda_1^{-1}\lambda_2 < 1$$

if and only if

$$\arctan\left(\frac{2+\sqrt{3\,\mu^2+4}}{3\mu}\right) < \theta_1.$$

By combining this expression with (12) for θ_1, a lengthy calculation then shows, for general α, that $\lambda_1^{-1}\lambda_2 < 1$ if and only if (16) holds. The eigenvectors associated with λ_1 and λ_2 are

$$(1-\lambda_1^{-1}\lambda_2, -\lambda_1^{-1}(\phi_1^+)^2)^T = (1-\xi, s)^T \quad \text{and} \quad (0,1)^T,$$

using (19) and (20), respectively. ∎

Remark 2. The main results in Proposition 1 were given in Génot and Brogliato [19], except for the inequality (16), which does not seem to have appeared in the literature before.[7] When $\mu = \mu_C(\alpha)$, it can be shown that $\tan\theta_1 = \sqrt{\frac{\alpha+1}{3}}$. From (11) and (16), we have

$$\mu_C = \frac{2}{\sqrt{3}}\mu_P \quad \forall\,\alpha, \tag{25}$$

independent of α. See also [44, Proposition 4.3].

Remark 3. Since $p_+ < 0$ within $\mathcal{F}$, the new time τ reverses direction there. Therefore the manifold γ^s gives a solution of (10) with respect to the original time having a smooth continuation through the singularity P (as indicated in Figure 2). We shall refer to this as a *strong singular canard*.

Remark 4. For $\mu_P < \mu < \mu_C$ so that $\xi > 1$, the direction $\theta = \theta_1$ is strong while (18) is weak. However, by evaluating the slope of the curve $b(\theta,\phi) = 0$ at the point P and comparing the result with $s/(1-\xi)$, it is straightforward to show that the weak eigendirection (18) is not contained within $\mathcal{F}\cup P\cup\mathcal{T}$. The reduced problem is only defined within $\mathcal{F}\cup\mathcal{T}$ and hence the classical Painlevé problem does therefore not support *weak singular canards*.

The implications of Proposition 1 are as follows. The dynamics cannot cross $p_+ = 0$ unless also $b = 0$. Furthermore, initial conditions within $\mathcal{L}$, as defined in (21), lift off at $b(\theta,\phi) = 0$. On the other hand, orbits within $\mathcal{S}$, defined in (22), are tangent to $p_+(\theta,\phi) = 0$ at P. Therefore the equilibrium value of the normal component of the contact force F_N, given in (9), becomes singular as (θ,ϕ) approaches P. Indeed, close to $P \equiv (\theta_1,\phi_1^+)$ we have

$$F_N \approx \frac{\partial_\theta b(\theta_1,\phi_1^+)(\theta-\theta_1)+\partial_\phi b(\theta_1,\phi_1^+)(\phi-\phi_1^+)}{\partial_\theta p_+(\theta_1)(\theta-\theta_1)} = \frac{\partial_\theta b(\theta_1,\phi_1^+)}{\partial_\theta p_+(\theta_1)} + \frac{\partial_\phi b(\theta_1,\phi_1^+)}{\partial_\theta p_+(\theta_1)}\frac{(\phi-\phi_1^+)}{(\theta-\theta_1)} \to \infty,$$

as $(\theta,\phi)\to P = (\theta_1,\phi_1^+)$ through the forward flow of [10]. But since $q_+ < 0$ in (6) near $p_+ = 0$, there exists a time T where $v(T) = 0$. Sufficiently close to P within $\mathcal{T}$, where F_N is

[7] The result $\mu_C(3) = \frac{8}{3\sqrt{3}}$ *does* appear in [19].

large, we will also have that $\dot{v} \lessgtr 0$ for $v = 0^{\pm}$, respectively. Hence sticking ($\dot{v} = 0$) occurs, as described by the Filippov vector-field [18].

As mentioned in the introduction, the rigid body equations (2) are unable to address what happens beyond P. Therefore we will now relax the rigid body assumption by adding compliance.

2.2. Compliance-based method. Following [14, 38], we assume that there are small excursions (compliance) into $y < 0$ in the neighborhood of the point A between the rod and the surface, when they are in contact (see Figure 1). Then we assume that the nonnegative normal force F_N takes the form

$$F_N(y,w) = \left[\varepsilon^{-1}F(\varepsilon^{-1}y,w)\right] = \begin{cases} 0 & \text{for} \quad y > 0, \\ \max\{\varepsilon^{-1}F(\varepsilon^{-1}y,w),0\} & \text{for} \quad y \le 0 \end{cases} \tag{26}$$

for $\varepsilon > 0$, where the operation $[\cdot]$ is defined by the last equality and F is assumed to be smooth with

$$F(\hat{y},w) = -\hat{y} - \delta w + \mathcal{O}((\hat{y}+w)^2). \tag{27}$$

The motivation for (26) is as follows. $F_N = 0$ for $y > 0$ because the rod is not in contact with the surface. The quantities $\lim_{y\to 0^-}(-\partial_y F_N(y,0)) = \varepsilon^{-2}$ and $\lim_{y\to 0^-}(-\partial_w F_N(y,0)) = \varepsilon^{-1}\delta$ represent a (scaled) spring constant and damping coefficient. This choice of scaling ensures [14, 38] that the critical damping coefficient is independent of ε. We are interested in the case when the compliance is very small, so we consider $0 < \varepsilon \ll 1$.

The first two equations in (6) play no role in what follows, so we drop them. Then we combine the remaining four equations in (6) with (26) to give the following set of governing equations, valid while $v > 0$, that we will use in what follows:

$$\begin{aligned} \dot{y} &= w, \\ \dot{w} &= b(\theta,\phi) + p_+(\theta)[\varepsilon^{-1}F(\varepsilon^{-1}y,w)], \\ \dot{\theta} &= \phi, \\ \dot{\phi} &= c_+(\theta)[\varepsilon^{-1}F(\varepsilon^{-1}y,w)]. \end{aligned} \tag{28}$$

In our previous paper [21], we studied this singularly perturbed system in the regions corresponding to the first (purple) $\mathcal{F}$ and fourth (green) "quadrants" of Figure 2 and showed the appearance of IWC. This provides further evidence that the scaling of the damping in (27) is the right one: as $\delta \to \infty$ IWC vanishes. In this paper, we consider the third (yellow) "quadrant" $\mathcal{T}$ and focus on the fate of P and γ^s under regularization.

2.3. Slow-fast analysis. To analyze (28) we consider the scaling

$$y = \varepsilon^2 y_2, \quad w = \varepsilon w_2, \tag{29}$$

also used in [21]. Inserting this into (28), with (27), gives a (2+2)-slow-fast system

$$\begin{aligned} \dot{y}_2 &= w_2, \\ \dot{w}_2 &= b(\theta,\phi) + p_+(\theta)\left[-y_2 - \delta w_2 + \varepsilon N(y_2,w_2,\varepsilon)\right], \\ \dot{\theta} &= \varepsilon\phi, \\ \dot{\phi} &= \varepsilon c_+(\theta)\left[-y_2 - \delta w_2 + \varepsilon N(y_2,w_2,\varepsilon)\right], \end{aligned} \tag{30}$$

upon scaling time by ε, where $N(y_2, w_2, \varepsilon) = \mathcal{O}((y_2 + w_2)^2 + \varepsilon(y_2 + w_2)^3)$ represents higher order terms. Setting $\varepsilon = 0$ gives the *layer problem*

$$\begin{aligned} \dot{y}_2 &= w_2, \\ \dot{w}_2 &= b(\theta, \phi) + p_+(\theta)\left[-y_2 - \delta w_2\right], \\ \dot{\theta} &= 0, \\ \dot{\phi} &= 0, \end{aligned} \tag{31}$$

in which both θ, ϕ are constant. Undoing the scaling of time by ε and then setting $\varepsilon = 0$ gives the *reduced problem*:

$$\begin{aligned} 0 &= w_2, \\ 0 &= b(\theta, \phi) + p_+(\theta)\left[-y_2 - \delta w_2\right], \\ \dot{\theta} &= \phi, \\ \dot{\phi} &= c_+(\theta)\left[-y_2 - \delta w_2\right]. \end{aligned} \tag{32}$$

The reduced problem is only defined on the critical points of the layer problem.

We now discuss some dynamics of both problems, summarized in Proposition 5 below. Let

$$g(\theta, \phi) = \frac{b(\theta, \phi)}{p_+(\theta)}, \quad (\theta, \phi) \in \mathcal{T} \cup \mathcal{F}, \tag{33}$$

where $\mathcal{F}$, $\mathcal{T}$ are defined in (14). Then we have the following.

Proposition 5. *The critical set S of the layer problem $(30)_{\varepsilon=0}$ is given by*

$$S = S_a \cup S_r \cup \widehat{P}$$

with

$$\begin{aligned} S_a: &\quad w_2 = 0,\ y_2 = g(\theta, \phi), \quad (\theta, \phi) \in \mathcal{T}, \\ S_r: &\quad w_2 = 0,\ y_2 = g(\theta, \phi), \quad (\theta, \phi) \in \mathcal{F}, \\ \widehat{P}: &\quad w_2 = 0,\ y_2 \in \mathbb{R},\ (\theta, \phi) = P. \end{aligned} \tag{34}$$

Here S_a is normally hyperbolic and attracting (focus-type), S_r is normally hyperbolic and repelling (saddle-type), while $\widehat{P}$ is a line of nonhyperbolic BT fixed points. The reduced flow on $S_{a,r}$ coincides with (10). In particular, if (16) holds, then γ^s, given in the (θ, ϕ)-plane by (17), is a solution to the reduced problem (32) having a smooth continuation through P.

Proof. The proof is straightforward. Linearization of the layer problem (31) about $w_2 = 0$, $y_2 = g(\theta, \phi)$, $(\theta, \phi) \in \mathcal{T} \cup \mathcal{F}$, from (34), gives

$$\begin{pmatrix} 0 & 1 \\ -p_+(\theta) & -p_+(\theta)\delta \end{pmatrix}.$$

Here we have used that $[F] = F$ when $F > 0$ and $y_2 < 0$; see (26). The PWS system (31) is therefore smooth in a neighborhood of any point on $S_{a,r}$. The eigenvalues are

$$\lambda_\pm = -\frac{1}{2}p_+(\theta)\delta \pm \frac{1}{2}\sqrt{-4p_+(\theta) + \delta^2 p_+(\theta)}.$$

Expansion about $\theta = \theta_1$, defined in (12), gives

$$\lambda_\pm = -\frac{1}{2}p'_+(\theta_1)\delta\Delta\theta(1 + \mathcal{O}(\Delta\theta)) \pm \frac{1}{2}\sqrt{-4p'_+(\theta)\Delta\theta(1 + \mathcal{O}(\Delta\theta))}, \tag{35}$$

where $\Delta\theta = \theta - \theta_1$ and then, since $p'_+(\theta_1) < 0$, the claims concerning $S_{a,r}$ therefore follow. Similarly, the linearization about any point in $\widehat{P}$ gives a nilpotent 2×2 Jordan block.

Inserting $w_2 = 0$, $y_2 = g(\theta, \phi)$ into (32) gives (10). The result therefore follows from Proposition 1. ∎

The strong singular canard γ^s connects S_a with S_r through $\widehat{P}$. It intersects $\widehat{P}$ in

$$\gamma^s \cap \widehat{P}: \quad y_2 = \frac{\partial_\theta b(\theta_1, \phi_1^+) + \partial_\phi b(\theta_1, \phi_1^+)(1-\xi)^{-1}s}{\partial_\theta p_+(\theta_1)},\ w_2 = 0,\ \theta = \theta_1,\ \phi = \phi_1^+,$$

using (17), (33), and (34). Note again (recall Remark 4) that, as opposed to the folded node in classical (2+1)-slow-fast systems [52, 55], there is no equivalent weak canard in this particular setting. Here the weak direction, defined by $\theta = \theta_1$, is an invariant of the reduced problem (23) but corresponds to $y_2 = -\infty$ by (33) and (34).

By Fenichel's theory [15, 16, 17], compact subsets of $S_{a,r}$ perturb to invariant slow manifolds $S_{a,\varepsilon}$ and $S_{r,\varepsilon}$, respectively. These objects are nonunique but $\mathcal{O}(e^{-c/\epsilon})$-close.

3. Main result.

Since the rigid body equations (2) are unable to address what happens beyond P, we introduced compliance in section 2.2, leading to a regularized set of governing equations (30). We have already seen in Proposition 5 that the point P becomes the line $\widehat{P}$ of nonhyperbolic BT points under regularization. Now we focus on the fate of the strong singular canard γ^s, also described in Proposition 5, under this regularization. For convenience, we summarize our main result here.

Theorem 6. *Suppose $\mu > \mu_C$ with μ_C as in (16) and consider a small neighborhood $\mathcal{U} \subset \{(\theta, \phi) \in \mathbb{R}^2\}$ of the point $P = (\theta_1, \phi_1^+)$, where $b = p_+ = 0$. Then for $0 < \varepsilon \leq \varepsilon_0$ sufficiently small there exists a* canard *orbit γ_ϵ^s of (30) connecting the attracting Fenichel slow manifold $S_{a,\varepsilon}$ with the stable manifold of the repelling Fenichel slow manifold $S_{r,\varepsilon}$. γ_ε^s is $o(1)$-close to γ^s within $\mathcal{U}$ and it divides $S_{a,\varepsilon}$ into orbits that lift off from those that eventually stick.*

Remark 7. We can estimate the $o(1)$ in Theorem 6 to be $\mathcal{O}(\varepsilon^{\eta(7-2\xi)/24})$ for any $\eta \in (0, 1)$, using Gronwall's inequality. This is a corollary of Proposition 25 in Appendix B. The estimate could probably be improved but we did not pursue this.

Remark 8. For the last statement of the theorem, we add the following. Fix $C > 0$ large and consider the following box in the (y_2, w_2, θ, ϕ)-space:

$$U = \{(y_2, w_2, \theta, \phi) \in \mathbb{R}^4 | y_2 \in [-C, 0],\ w_2 \in [-\varpi^{-1}, \varpi^{-1}],\ (\theta, \phi) \in [\theta_1 - \chi, \theta_1 + \chi] \times [\phi_1^+ - \chi, \phi_1^+ + \chi]\},$$

with $\varpi > 0$ and $\chi > 0$ both sufficiently small. Fenichel's manifold $S_{a,\varepsilon}$ is a graph over compact domains $\mathcal{C} \subset \mathcal{T}$. Within $\mathcal{C}$ we can write γ_ε^s as

$$\phi = m_{ss,\varepsilon}(\theta) = m_{ss}(\theta) + o(1);$$

recall (17). Now, consider initial conditions on the intersection of $S_{a,\varepsilon}$ with the subset of the $\{\theta = \theta_1 - \chi\}$-face of the box U, where ϕ is sufficiently close but greater than $m_{ss,\varepsilon}(\theta_1 - \chi)$. Under the forward flow, points within this set will then either leave the box U through its $\{\theta = \theta_1 + \chi\}$-face, if ϕ is $\mathcal{O}(e^{-c/\varepsilon})$-close to $m_{ss,\varepsilon}(\theta_1 - \chi)$, or leave the box U through the $\{y_2 = 0\}$-face with $w_2 > 0$ such that lift-off occurs (like $\mathcal{L}$ in Proposition 1). Similarly, consider initial conditions on the intersection of $S_{a,\varepsilon}$ with the subset of the $\{\theta = \theta_1 - \chi\}$-face of the box U, where ϕ is sufficiently close but less than $m_{ss,\varepsilon}(\theta_1 - \chi)$. Under the foward flow, points within this set will then either leave the box U through its $\{\theta = \theta_1 + \chi\}$-face, if ϕ is $\mathcal{O}(e^{-c/\varepsilon})$-close to $m_{ss,\varepsilon}(\theta_1 - \chi)$, or leave the box U through the $\{y_2 = -C\}$-face with $w_2 < 0$ such that sticking and IWC occurs (like $\mathcal{S}$ in Proposition 1), as described in [21].

These results are corollaries of Theorem 1 and Fenichel's theory and they generalize Proposition 1 to the compliant version. Note that orbits initially on the Fenichel slow manifold $S_{a,\varepsilon}$ do not twist upon passage near $\widehat{P}$. In particular, the projection of orbits on $S_{a,\varepsilon}$ near γ_ε^s onto the (y_2, w_2)-plane do not oscillate. This is part of our main result. It is clearly different when we go backward from $S_{r,\varepsilon}$ because S_a is of focus-type. Consider initial conditions on the intersection of $S_{r,\epsilon}$ with the subset of the $\{\theta = \theta_1 + \chi\}$-face of U, where ϕ is sufficiently close to $\phi = m_{ss,\varepsilon}(\theta_1 + \chi)$. These points will under the backward flow have projections onto the (y_2, w_2)-plane that oscillate around γ_ε^s when reaching $\mathcal{T}$.

In the next section, to begin the proof of Theorem 6, in (36) we present a rescaled version of (30) in order to simplify the subsequent blowup of $\widehat{P}$ in section 4.1. Our approach naturally leads to three different changes of variable, known as *charts*, which are analyzed in sections 4.4 to 4.6. The technical details are presented in a series of appendices.

4. Proof of Theorem 6. Starting with (30) we proceed by (a) dropping the subscripts on (y, w), (b) moving $P = (\theta_1, \phi_1^+)$ to the origin $(\theta, \phi) = 0$, (c) straightening out the zero level set of b to $\phi = 0$, (d) eliminating time, and finally (e) applying appropriate scalings. Omitting the details, we obtain the system

$$\begin{aligned} \varepsilon y' &= (1 + f(\theta, \phi))w, \\ \varepsilon w' &= \phi(1 + \tilde{b}(\theta, \phi)) - \theta(1 + \tilde{p}(\theta, \phi))\left[-y - \delta w + \varepsilon N(y, w)\right], \\ \theta' &= 1, \\ \phi' &= \xi(1 + \tilde{c}(\theta, \phi))\left[-y - \delta w + \varepsilon N(y, w)\right] + s(1 + h(\theta)) \end{aligned} \tag{36}$$

for $(\theta, \phi) \in \mathcal{U}$, a small neighborhood of $(0, 0)$, where $\xi \in (0, 1), s > 0$ are defined in (19) and (20), where

$$\begin{aligned} f(\theta, \phi) &= \mathcal{O}(\theta + \phi), \\ h(\theta) &= \mathcal{O}(\theta), \end{aligned}$$

and

$$\tilde{b}(\theta,\phi) = \mathcal{O}(\theta+\phi),$$
$$\tilde{p}(\theta,\phi) = \mathcal{O}(\theta+\phi),$$
$$\tilde{c}(\theta,\phi) = \mathcal{O}(\theta+\phi)$$

are all smooth functions. For simplicity, we suppress any dependency on ε, since this will play no role in the following. Also, since we will be working near γ^s on $S_{a,r}$ the nonsmoothness of F_N will play no role in the following. We will therefore replace $[\cdot]$ in (36) by parentheses; recall (26).

We will now prove the existence of a strong canard for (36) for $0 < \epsilon \ll 1$, which then proves Theorem 6. We begin by redefining the sets $\mathcal{F}$ and $\mathcal{T}$ from (14) as

$$\mathcal{F} = \mathcal{U} \cap \{\theta > 0,\, \phi > 0\},$$
$$\mathcal{T} = \mathcal{U} \cap \{\theta < 0,\, \phi < 0\},$$

so that they are now precisely the first and third quadrant, respectively, of the (θ,ϕ)-plane. We also redefine $g(\theta,\phi)$ from (33) as

$$g(\theta,\phi) = -\frac{\phi(1+\tilde{b}(\theta,\phi))}{\theta(1+\tilde{p}(\theta,\phi))}, \quad (\theta,\phi) \in \mathcal{F} \cup \mathcal{T}; \tag{37}$$

then the critical set S of the layer problem $(36)_{\epsilon=0}$ is a union of

$$\begin{aligned} S_a: &\quad w = 0,\, y = g(\theta,\phi), \quad (\theta,\phi) \in \mathcal{T}, \\ S_r: &\quad w = 0,\, y = g(\theta,\phi), \quad (\theta,\phi) \in \mathcal{F}, \\ \widehat{P}: &\quad y \in \mathbb{R},\, w = \theta = \phi = 0, \end{aligned} \tag{38}$$

identical to (34). Following arguments identical to those used in Proposition 5, S_a is normally hyperbolic and attracting (focus-type), S_r is normally hyperbolic and repelling (saddle-type), and $\widehat{P}$ is a line of nonhyperbolic BT points, as before. Finally, there exists a strong singular canard γ^s for the slow flow on $S_a \cup S_r$ that is tangent to

$$(1-\xi, s)^T, \tag{39}$$

at $(\theta,\phi) = 0$, in the (θ,ϕ)-plane. Using (37) it follows that γ^s on S intersects $\widehat{P}$ in

$$y = -(1-\xi)^{-1}s,\, w = \theta = \phi = 0. \tag{40}$$

Compact 2D submanifolds (with boundaries) of S_a and S_r perturb by Fenichel's theory [15, 16, 17] to attracting and repelling invariant manifolds $S_{a,\varepsilon}$ and $S_{r,\varepsilon}$, respectively, for ϵ sufficiently small.

We now blow up the line $\widehat{P}$, defined in (38), using the formalism of Krupa and Szmolyan [28].

4.1. Blowup of $\widehat{P}$. To study system (36) near $\widehat{P}$ we consider the extended system $((36), \varepsilon' = 0)$ written in terms of the fast time scale:

$$
\begin{aligned}
\dot{y} &= (1 + f(\theta, \phi))w, \\
w' &= \phi(1 + \tilde{b}(\theta, \phi)) - \theta(1 + \tilde{p}(\theta, \phi))\left[-y - \delta w + \varepsilon N(y, w)\right], \\
\dot{\theta} &= \varepsilon, \\
\dot{\phi} &= \varepsilon\left(\xi(1 + \tilde{c}(\theta, \phi))\left[-y - \delta w + \varepsilon N(y, w)\right] + s(1 + h(\theta))\right), \\
\dot{\varepsilon} &= 0.
\end{aligned} \tag{41}
$$

In this way, S_a, S_r, and $\widehat{P}$ become subsets of $\{\epsilon = 0\}$. Similarly, the Fenichel 2D slow manifolds $S_{a,\varepsilon}$ and $S_{r,\varepsilon}$ are now $\{\varepsilon = \text{const.}\}$-sections of 3D center manifolds M_a and M_r of (41). We will continue to denote these obvious embeddings by the same symbols.

We will work in a small neighborhood of $\widehat{P}: y \in (-\infty, 0], (w, \theta, \phi, \varepsilon) = 0$ We then apply the following blowup of $(w, \theta, \phi, \varepsilon) = 0$,

$$
\Phi: \quad (y, r, (\bar{w}, \bar{\theta}, \bar{\phi}, \bar{\epsilon})) \in \mathcal{B} \to (y, w, \theta, \phi, \varepsilon) \in \mathbb{R}^4 \times \mathbb{R}_+, \quad \mathcal{B} \equiv \mathbb{R} \times R_+ \times S^3,
$$

defined by

$$
w = r\bar{w}, \quad \theta = r^2\bar{\theta}, \quad \phi = r^2\bar{\phi}, \quad \varepsilon = r^3\bar{\epsilon} \tag{42}
$$

with

$$
S^3: \quad \bar{w}^2 + \bar{\theta}^2 + \bar{\phi}^2 + \bar{\epsilon}^2 = 1.
$$

The blowup map Φ does not change y so we retain this symbol. Notice that $r = 0$ in (42) corresponds to $\widehat{P}$ and Φ therefore blows up $\widehat{P}$ to a cylinder of 3-spheres $(y, (\bar{w}, \bar{\theta}, \bar{\phi}, \bar{\epsilon})) \in (-\infty, 0] \times S^3$.

The mapping Φ gives rise to a vector-field $\overline{X}$ on $\mathcal{B}$ by pull-back of (41). Here $\overline{X}|_{r=0} = 0$. The exponents (or weights) of r in (42) are, however, chosen so that the desingularized vector-field

$$
\widehat{X} = r^{-1}\overline{X}
$$

is well-defined and nontrivial for $r = 0$. It is $\widehat{X}$ that we shall study in what follows. As usual, the orbits of $\widehat{X}$ agree with those of $\overline{X}$ for $r > 0$ but the fact that $\widehat{X}$ is nontrival for $r = 0$ allows us to use regular perturbation techniques to describe $\overline{X}$ for r small.

4.2. Charts. Clearly, we can describe a small neighborhood of $(w, \theta, \phi, \varepsilon) = 0$ with $\varepsilon \geq 0$ by studying each value of $(r, (\bar{w}, \bar{\theta}, \bar{\phi}, \bar{\epsilon}))$ with $r \sim 0$ and with $(\bar{w}, \bar{\theta}, \bar{\phi}, \bar{\epsilon}) \in S^3 \cap \{\bar{\epsilon} \geq 0\}$. Instead of working with spherical coordinates, it is more convenient to work with the directional charts

$$
\kappa_1: \ \bar{\theta} = -1: \quad w = r_1 w_1, \quad \theta = -r_1^2, \quad \phi = r_1^2\phi_1, \quad \varepsilon = r_1^3\epsilon_1, \quad (w_1, \phi_1, \epsilon_1) \in K_1, \tag{43}
$$

$$
\kappa_2: \ \bar{\epsilon} = 1: \quad w = r_2 w_2, \quad \theta = r_2^2\theta_2, \quad \phi = r_2^2\phi_2, \quad \varepsilon = r_2^3, \quad (w_2, \theta_2, \phi_2) \in K_2, \tag{44}
$$

$$
\kappa_3: \ \bar{\theta} = 1: \quad w = r_3 w_3, \quad \theta = r_3^2, \quad \phi = r_3^2\phi_3, \quad \varepsilon = r_3^3\epsilon_3, \quad (w_3, \phi_3, \epsilon_3) \in K_3, \tag{45}
$$

that correspond to setting $\bar{\theta} = -1$, $\bar{\epsilon} = 1$, and $\bar{\theta} = 1$, respectively, in (42). The sets K_1, K_2, and K_3 are sufficiently large open sets in $\mathbb{R}^3$ so that the three charts cover our neighborhood of $(w, \theta, \phi, \varepsilon) = 0$ with $\varepsilon \geq 0$. In the proof of Theorem 6, we will actually fix K_1 and K_3 to be such that the boxes

$$U_1 = \{(w_1, \phi_1, \epsilon_1) \in \mathbb{R}^3 | w_1 \in [-\sigma, \sigma],\ \epsilon_1 \in [0, \nu]\ \phi_1 \in [-\varpi^{-1}, -\varpi]\}, \tag{46}$$

$$U_3 = \{(w_3, \phi_3, \epsilon_3) \in \mathbb{R}^3 | w_3 \in [-\sigma, \sigma],\ \epsilon_3 \in [0, \nu]\ \phi_3 \in [\varpi, \varpi^{-1}]\} \tag{47}$$

for $\sigma > 0$, $\nu > 0$, and $\varpi > 0$ sufficiently small are subsets of K_1 and K_3, respectively, and then adjust K_2 accordingly. In particular, we will take K_2 so large that the box

$$\begin{aligned} U_2 = \{(w_2, \theta_2, \phi_2) \in \mathbb{R}^3 | w_2 \in [-\nu^{-1/3}\sigma, \nu^{-1/3}\sigma],\ \theta_2 \in [-\nu^{-2/3}, \nu^{-2/3}], \\ \phi_2 \in [-\nu^{-2/3}\varpi^{-1}, \nu^{-2/3}\varpi^{-1}]\} \end{aligned} \tag{48}$$

is a subset of K_2.

The chart κ_1 is called the *entry chart*, κ_2 is called the *scaling chart*, and finally κ_3 is called the *exit chart*. Geometrically (43) can be interpreted as a stereographic-like projection from the plane $\{(w_1, -1, \phi_1, \epsilon_1) | (w_1, \phi_1, \epsilon_1) \in K_1\}$, tangent to S^3 at $\bar{\theta} = -1$, to the hemisphere $S^3 \cap \{\bar{\theta} < 0\}$:

$$w_1 = (-\bar{\theta})^{-1/2}\bar{w}, \quad \phi_1 = (-\bar{\theta})^{-1}\bar{\phi}, \quad \epsilon_1 = (-\bar{\theta})^{-3/2}\bar{\epsilon}.$$

Similar interpretations apply to (44) and (45):

$$\begin{aligned} w_2 &= \bar{\epsilon}^{-1/3}\bar{w}, \quad \theta_2 = \bar{\epsilon}^{-2/3}\bar{\theta}, \quad \phi_2 = \bar{\epsilon}^{-2/3}\bar{\phi}, \\ w_3 &= \bar{\theta}^{-1/2}\bar{w}, \quad \phi_3 = \bar{\theta}^{-1}\bar{\phi}, \quad \epsilon_3 = \bar{\theta}^{-3/2}\bar{\epsilon} \end{aligned}$$

for $\bar{\epsilon} > 0$ and $\bar{\theta} > 0$, respectively. We follow the convention that variables, manifolds, and other dynamical objects will be given a subscript i in chart κ_i. Similarly, objects in the blowup variables $(y, r, (\bar{w}, \bar{\theta}, \bar{\phi}, \bar{\epsilon}))$ are given an overline.

4.3. Coordinate changes. When the charts κ_1 and κ_2 or κ_2 and κ_3 overlap we can change coordinates. (κ_1 and κ_3 cannot overlap.) We will denote the smooth change of coordinates from κ_i to κ_j by κ_{ji}. Straightforward calculations show that

$$\begin{aligned} \kappa_{12}: \quad (r_2, w_2, \theta_2, \phi_2) &\mapsto (r_1, w_1, \phi_1, \epsilon_1), \\ r_1 &= r_2(-\theta_2)^{1/2}, \\ w_1 &= (-\theta_2)^{-1/2}w_2, \\ \phi_1 &= (-\theta_2)^{-1}\phi_2, \\ \epsilon_1 &= (-\theta_2)^{-3/2} \end{aligned} \tag{49}$$

for $r_2 \geq 0$ and all $(w_2, \theta_2, \phi_2) \in K_2$ so that $(w_1, \phi_1, \epsilon_1) \in K_1$. Furthermore,

$$\begin{aligned}\kappa_{23}: \quad (r_3, w_3, \phi_3, \epsilon_3) &\mapsto (r_2, w_2, \theta_2, \phi_2),\\ r_2 &= r_3 \epsilon_3^{1/3},\\ w_2 &= \epsilon_3^{-1/3} w_3,\\ \theta_2 &= \epsilon_3^{-2/3},\\ \phi_2 &= \epsilon_3^{-2/3} \phi_3\end{aligned}$$

for $r_3 \geq 0$ and all $(w_3, \phi_3, \epsilon_3) \in K_3$ so that $(w_1, \phi_1, \epsilon_1) \in K_1$. The expressions for κ_{21} and κ_{32} follow easily from these results. Notice, in particular, that

$$\kappa_{23}(r_3, w_3, \phi_3, \nu) = (r_3 \nu^{1/3}, \nu^{-1/3} w_3, \nu^{-2/3}, \nu^{-2/3} \phi_3)$$

and hence the $\{\epsilon_3 = \nu\}$-face of the box U_3 (47) gets mapped by the diffeomorphism κ_{23} to a subset of the $\{\theta_2 = \nu^{-2/3}\}$-face of the box U_2 (48). Similarly, the $\{\epsilon_1 = \nu\}$-face of U_1 (46) gets mapped by the diffeomorphism κ_{12} to a subset of the $\{\theta_2 = -\nu^{-2/3}\}$-face of U_2. We collect this result in the following lemma.

Lemma 9.

$$\begin{aligned}\kappa_{23}\left(\{\epsilon_3 = \nu\} \cap U_3\right) &= \{\theta_2 = \nu^{-2/3},\ \phi_2 \in [\nu^{-2/3}\varpi, \nu^{-2/3}\varpi^{-1}]\} \cap U_2,\\ \kappa_{21}\left(\{\epsilon_1 = \nu\} \cap U_1\right) &= \{\theta_2 = -\nu^{-2/3},\ \phi_2 \in [-\nu^{-2/3}\varpi^{-1}, -\nu^{-2/3}\varpi]\} \cap U_2.\end{aligned}$$

In chart κ_1 we will encounter a line of normally *elliptic* critical points. A true unfolding of $\widehat{P}$ as a line of co-dimension two BT-bifurcation points, similar to the approach in [7], would enable some hyperbolicity in this chart (without the need for additional blowup). However, for our problem such an unfolding is unphysical. Instead we will apply a sequence of normal form transformations that accurately eliminates the fast oscillations, and then subsequently apply an additional blowup that captures the contraction in the entry chart, enabling an accurate continuation of the slow manifold into the scaling chart κ_2 and the $\{\theta_2 = -\nu^{-2/3}\}$-face of U_2.

Due to the technical difficulties in chart κ_1 in this paper we will work our way backward, starting from the exit chart κ_3 in section 4.4, then move onto the scaling chart κ_2 in section 4.5, and then finally attack the difficulties in the entry chart κ_1 in section 4.6. Lengthy proofs are consigned to a series of appendices. Then, in section 4.7 we combine these results to prove Theorem 6.

4.4. Exit chart κ_3. Substituting (45) into (36) gives

$$\begin{aligned}\dot{y} &= (1 + r_3^2 f_3(r_3, \phi_3)) w_3,\\ \dot{w}_3 &= \phi_3(1 + r_3^2 b_3(r_3, \phi_3)) - (1 + r_3^2 p_3(r_3, \phi_3))\left(-y - \delta r_3 w_3 + \varepsilon N(y, r_3 w_3, \varepsilon)\right) - \frac{1}{2}\epsilon_3 w_3,\\ \dot{r}_3 &= \frac{1}{2} r_3 \epsilon_3,\\ \dot{\epsilon}_3 &= -\frac{3}{2}\epsilon_3^2,\\ \dot{\phi}_3 &= \epsilon_3\left(\xi(1 + r_3^2 g_3(r_3, \phi_3))\left(-y - \delta r_3 w_3 + \varepsilon N(y, r_3 w_3, \varepsilon)\right) + s(1 + r_3^2 h_3(r_3, \phi_3)) - \phi_3\right),\end{aligned}$$

after division of the right-hand side by r_3. We keep the use of ε $(= r_3^3 \epsilon_3)$ for brevity.

The subspaces $\{r_3 = 0\}$ and $\{\epsilon_3 = 0\}$ are invariant. Along their intersection $\{r_3 = \epsilon_3 = 0\}$ we find

$$L_3 : \quad y = \phi_3,\ w_3 = r_3 = \epsilon_3 = 0,$$

as a line of critical points. Linearizing about a point in L_3 gives the following generalized eigensolutions (λ_i, w_i):

$$\lambda_1 = 1, \quad w_1 = (1,1,0,0,0)^T, \quad \lambda_2 = -1, \quad w_2 = (1,-1,0,0,0)^T$$

and

$$\lambda_{3,4,5} = 0, \quad w_{3,4,5} = (0,0,1,0,0)^T, (-1,0,1,0,0)^T, (0,0,0,0,1)^T.$$

Hence we have gained hyperbolicity of S_r at the blowup of P. Now, consider the set

$$V_3 = \{(y, r_3, (w_3, \phi_3, \epsilon_3)) \in (-\infty, 0] \times [0, \nu] \times U_3\}$$

with U_3 as in (47). In particular, we shall henceforth fix $\varpi > 0$ small enough so that $\phi_3 = (1-\xi)^{-1}s \in [\varpi, \varpi^{-1}]$. Then we have the following proposition.

Proposition 10. *For ν sufficiently small, there exists a smooth saddle-type center manifold within V_3:*

$$\begin{aligned} M_{r,3} : \quad & y = -\phi_3 + \epsilon_3^2(s-(1-\xi)\phi_3)(1+\epsilon_3\psi_1^{(y)}(\phi_3,\epsilon_3)) + r_3\psi_2^{(y)}(r_3,\phi_3,\epsilon_3), \\ & w_3 = \epsilon_3(s-(1-\xi)\phi_3)(1+\epsilon_3\psi_1^{(w)}(\phi_3,\epsilon_3)) + r_3\psi_2^{(w)}(r_3,\phi_3,\epsilon_3), \end{aligned}$$

where

$$\psi_2^{(w)}(r_3,\phi_3,\epsilon_3),\ \psi_2^{(y)}(r_3,\phi_3,\epsilon_3) = \mathcal{O}(r_3+\epsilon_3).$$

Also locally, $M_{r,3}$ has smooth stable and unstable manifolds:

$$\begin{aligned} W^s(M_{r,3}) : \quad & y = m_s(w_3, r_3, \phi_3, \epsilon_3) = -\phi_3 - w_3 + \mathcal{O}(r_3+\epsilon_3), \\ W^u(M_{r,3}) : \quad & y = m_u(w_3, r_3, \phi_3, \epsilon_3) = -\phi_3 + w_3 + \mathcal{O}(r_3+\epsilon_3) \end{aligned}$$

with $m_{s,u}$ both smooth. The manifold $M_{r,3}$ contains $S_{r,3} \equiv \kappa_3(S_r)$ within $\epsilon_3 = 0$ as a set of critical points and

$$\begin{aligned} C_{r,3} : \quad & y = -\phi_3 + \epsilon_3^2(s-(1-\xi)\phi_3)(1+\epsilon_3\psi_1^{(y)}(\phi_3,\epsilon_3)), \\ & w_3 = \epsilon_3(s-(1-\xi)\phi_3)(1+\epsilon_3\psi_1^{(w)}(\phi_3,\epsilon_3)) \end{aligned}$$

within $r_3 = 0$, as a center saddle-type submanifold. The submanifold $C_{r,3}$ contains the invariant line:

$$l_3 : \quad y = -\frac{s}{1-\xi},\ w_3 = 0,\ \phi_3 = \frac{s}{1-\xi},\ \epsilon_3 \geq 0,\ r_3 = 0. \tag{50}$$

Proof. Follows from center manifold theory and simple calculations. ∎

The manifold $M_{r,3}$ is foliated by invariant hyperbolas $r_3^3\epsilon_3 = \varepsilon \geq 0$. We let

$$M_{r,3}(\varepsilon) \equiv M_{r,3} \cap \{\varepsilon = r_3^3\epsilon_3\}$$

with $0 < \varepsilon \ll 1$ fixed. It is an extension of the Fenichel slow manifold $S_{r,\varepsilon}$ up to $\{\epsilon_3 = \nu\}$-face of V_3. Here it is a smooth graph over ϕ_1 and $r_1 = (\varepsilon\nu^{-1})^{1/3}$:

$$\begin{aligned} M_{r,3}(\varepsilon) \cap \{\epsilon_3 = \nu\} : \quad y &= -\phi_3 + \nu^2(s - (1-\xi)\phi_3)(1 + \nu\psi_1^{(y)}(\phi_3, \nu)) \\ &\quad + (\varepsilon\nu^{-1})^{1/3}\psi_2^{(y)}((\varepsilon\nu^{-1})^{1/3}, \phi_3, \nu), \\ w_3 &= \nu(s - (1-\xi)\phi_3)(1 + \nu\psi_1^{(w)}(\phi_3, \nu)) \\ &\quad + (\varepsilon\nu^{-1})^{1/3}\psi_2^{(w)}((\varepsilon\nu^{-1})^{1/3}, \phi_3, \nu), \end{aligned} \tag{51}$$

where it is $\mathcal{O}(\varepsilon^{1/3})$-close to $C_{r,3} \cap \{\epsilon_3 = \nu\}$. The reduced problem on $M_{r,3}$ is

$$\begin{aligned} \dot{r}_3 &= \frac{1}{2}r_3, \\ \dot{\epsilon}_3 &= -\frac{3}{2}\epsilon_3, \\ \dot{\phi}_3 &= (s - (1-\xi)\phi_3)(1 + \mathcal{O}(\epsilon_3^2)) + r_3\mathcal{O}(\epsilon_3 + r_3), \end{aligned} \tag{52}$$

after division by ϵ_3. This division desingularizes the dynamics within $S_{r,3} \subset \{\epsilon_3 = 0\}$. The point

$$p_3 : \quad r_3 = \epsilon_3 = 0,\ \phi_3 = (1-\xi)^{-1}s > 0$$

is a hyperbolic equilibrium of the reduced problem (52). It is the intersection of $\bar{\gamma}^s$ with the blowup cylinder.[8] See (39) and (40). The linearization of (52) about p_3 gives eigenvalues $\frac{1}{2}$, $-(1-\xi)$, $-\frac{3}{2}$, respectively. The invariant line $l_3 : r_3 = 0, \phi_3 = (1-\xi)^{-1}s, \epsilon_3 \geq 0$ is therefore the strong stable manifold within $\{r_3 = 0\}$ of p_3 for the reduced problem (52), coinciding with the strong eigenvector associated with the strong eigenvalue $-\frac{3}{2} < -(1-\xi)$, since $\xi \in (0,1)$ from (19). The unique unstable manifold contained within the (r_3, ϕ_3)-plane corresponds to the singular strong canard $\kappa_3(\gamma^s) \subset \{\epsilon_3 = 0\}$. We will continue l_3 backward into chart κ_2 in the following section.

4.5. Scaling chart κ_2.

Substituting (44) into (36) gives

$$\begin{aligned} \dot{y} &= w_2, \\ \dot{w}_2 &= \phi_2(1 + r_2^2 b_2(\theta_2, \phi_2, r_2)) - \theta_2(1 + r_2^2 p_2(\theta_2, \phi_2, r_2))\left(-y - \delta r_2 w_2 + \varepsilon N(y, r_2 w_2, \varepsilon)\right), \\ \dot{\theta}_2 &= 1, \\ \dot{\phi}_2 &= \xi(1 + r_2^2 g_2(\theta_2, \phi_2, r_2))\left(-y - \delta r_2 w_2 + \varepsilon N(y, r_2 w_2, \varepsilon)\right) + s(1 + r_2^2 h_2(\theta_2, r_2)), \end{aligned} \tag{53}$$

[8] $\bar{\gamma}^s$ is simply γ^s in terms of the blowup variables $(y, (\bar{w}, \bar{\theta}, \bar{\phi}, \bar{\epsilon})) \in \mathbb{R} \times S^3$.

after division of the right-hand side by r_2. Also $\dot{r}_2 = 0$ since $r_2 = \varepsilon^{1/3}$. In this chart, we consider the set

$$V_2 = \{(y, r_2, (w_2, \theta_2, \phi_2)) \in (-\infty, 0] \times [0, \nu] \times U_2\}$$

with U_2 as in (48). Setting $r_2 = 0$ gives the following linear system:

$$\begin{aligned} y'(\theta_2) &= w_2, \\ w_2'(\theta_2) &= \phi_2 + \theta_2 y, \\ \phi_2'(\theta_2) &= -\xi y + s, \end{aligned} \tag{54}$$

after the elimination of time.

Lemma 11. *Recall $\xi \in (0,1)$. The line*

$$l_2 : \quad \phi_2 = \frac{s}{1-\xi}\theta_2, \quad y = -\frac{s}{1-\xi}, \quad w_2 = 0,\ \theta_2 \in \mathbb{R},\ r_2 = 0 \tag{55}$$

is an invariant of $(53)_{r_2=0}$. It coincides with $\kappa_{23}(l_3)$, where l_3 is the invariant line in chart κ_3, given in (50).

Proof. This is a straightforward calculation. ∎

Remark 12. Note that the projection of the line l_2 onto the (θ_2, ϕ_2) plane coincides with the span of the eigenvector in (39). In terms of the blowup variables $(y, (\bar{w}, \bar{\theta}, \bar{\phi}, \bar{\epsilon})) \in \mathbb{R} \times S^3$ it becomes the great circle

$$\bar{l} : \quad y = -\frac{s}{1-\xi}, \quad r = 0, \quad \bar{w} = 0, \quad \bar{\theta}^{-1}\bar{\phi} = \frac{s}{1-\xi}, \quad (\bar{\theta}, \bar{\phi}, \bar{\epsilon}) \in S^2.$$

We now show that (54) can be rewritten as Langer's [33, 34] equation (1). Let

$$\phi_2 = \frac{s}{1-\xi}\theta_2 + \tilde{\phi}_2, \quad y = -\frac{s}{1-\xi} + \tilde{y}, \tag{56}$$

which centers l_2 along $\tilde{y} = w_2 = \tilde{\phi}_2 = 0$. Then (54) becomes

$$\begin{aligned} \tilde{y}'(\theta_2) &= w_2, \\ w_2'(\theta_2) &= \tilde{\phi}_2 + \theta_2 \tilde{y}, \\ \tilde{\phi}_2'(\theta_2) &= -\xi \tilde{y}. \end{aligned} \tag{57}$$

We now eliminate w_2 and $\tilde{\phi}_2$ as

$$w_2(\theta_2) = \tilde{y}'(\theta_2), \quad \tilde{\phi}_2(\theta_2) = w_2'(\theta_2) - \theta_2\tilde{y}(\theta_2) = \tilde{y}''(\theta_2) - \theta_2\tilde{y}(\theta_2), \tag{58}$$

to finally obtain Langer's equation

$$\tilde{y}'''(\theta_2) = \theta_2\tilde{y}'(\theta_2) + (1-\xi)\tilde{y}(\theta_2). \tag{59}$$

The general solution of (59) can be expressed in terms of hyper-geometric functions. But we do not find this presentation useful. Instead we investigate those asymptotic properties of the solutions of (59) that are important for our analysis.

Lemma 13. *The solution space of* (59) *is spanned by the following linearly independent solutions:*

$$\mathrm{La}_\xi(\theta_2) = \int_0^\infty \exp\left(-\tau^3/3 + \theta_2\tau\right)\tau^{-\xi}d\tau, \tag{60}$$

$$\mathrm{Lb}_\xi(\theta_2) = \int_0^\infty \cos(\tau^3/3 + \theta_2\tau + \xi\pi/2)\tau^{-\xi}d\tau, \tag{61}$$

$$\mathrm{Lc}_\xi(\theta_2) = \int_0^\infty \cos(\tau^3/3 + \theta_2\tau - \xi\pi/2)\tau^{-\xi}d\tau. \tag{62}$$

Here span $\{\mathrm{La}_\xi\}$ *contains all* nonoscillatory solutions *of* (59) *for* $\theta_2 \to -\infty$. *The solution* La_ξ *can be written in the following form for* $\theta_2 < 0$*:*

$$\mathrm{La}_\xi = (-\theta_2)^{-(1-\xi)}E_2((-\theta_2)^{-3})$$

with E_2 *real analytic and satisfying*

$$E_2(0) = \Gamma(1-\xi),$$

where $\Gamma(z) = \int_0^\infty t^{z-1}e^{-t}dt$ *is the* Γ*-function. The following asymptotics hold:*

$$\mathrm{La}_\xi(\theta_2) = \sqrt{\pi}\theta_2^{(1-\xi)/2-3/4}\exp\left(2\theta_2^{3/2}/3\right)(1+o(1)), \tag{63}$$

$$\mathrm{Lb}_\xi(\theta_2) = \frac{\sqrt{\pi}}{2}\theta_2^{(1-\xi)/2-3/4}\exp\left(-2\theta_2^{3/2}/3\right)(1+o(1)), \tag{64}$$

$$\mathrm{Lc}_\xi(\theta_2) = \sin(\xi\pi)\theta_2^{(1-\xi)/2-3/2}\Gamma(1-\xi)(1+o(1)) \tag{65}$$

for $\theta_2 \to \infty$, *and*

$$\mathrm{La}_\xi(\theta_2) = (-\theta_2)^{-(1-\xi)}\Gamma(1-\xi)(1+\mathcal{O}(\theta_2^{-3})), \tag{66}$$

$$\mathrm{Lb}_\xi(\theta_2) = \sqrt{2\pi}(-\theta_2)^{(1-\xi)/2-3/4}\sin\left(\frac{2}{3}(-\theta_2)^{3/2}(1+o(1)) + \frac{\pi}{4} - \frac{\xi\pi}{2}\right)(1+o(1))$$

$$+ \sin(\xi\pi)\mathrm{La}_\xi(\theta_2), \tag{67}$$

$$\mathrm{Lc}_\xi(\theta_2) = \sqrt{2\pi}(-\theta_2)^{(1-\xi)/2-3/4}\sin\left(\frac{2}{3}(-\theta_2)^{3/2}(1+o(1)) + \frac{\pi}{4} + \frac{\xi\pi}{2}\right)(1+o(1)) \tag{68}$$

for $\theta_2 \to -\infty$.

Proof. We apply the Laplace transform $\tilde{y}(\theta) = \int_\Upsilon \hat{y}(z)e^{\theta z}dz$ and solve for $\hat{\tilde{y}}(z)$, $z \in D \subset \mathbb{C}$, and the unbounded contour $\Upsilon \subset D$. This representation simplifies the asymptotics for $\theta \to \pm\infty$. Full details are given in Appendix A. ∎

Remark 14. Note that $\mathrm{Lb}_0 = \mathrm{Lc}_0 = \pi\mathrm{Ai}$, where Ai is the standard Airy function. Also, from Lemma 13, the following hold:

- La_ξ has (a) algebraic decay and is nonoscillatory for $\theta_2 \to -\infty$ and (b) exponential growth for $\theta_2 \to \infty$.
- Lb_ξ has (a) oscillatory behavior for $\theta_2 \to -\infty$ and (b) exponential decay for $\theta_2 \to \infty$.
- Lc_ξ has (a) oscillatory behavior for $\theta_2 \to -\infty$ and (b) algebraic decay for $\theta_2 \to \infty$.

The oscillatory behavior for Lb_ξ and Lc_ξ for $\theta_2 \to -\infty$ decays in amplitude, since $(-\theta_2)^{(1-\xi)/2-3/4} \to 0$ for $\xi \in (0,1)$.

Given $\tilde{y}(\theta_2)$, the values of $(w_2, \tilde{\phi}_2)$ can be determined from (58). In particular, $\tilde{y} = \mathrm{La}_\xi(\theta_2)$ and $\tilde{y} = \mathrm{Lc}_\xi(\theta_2)$ give $(w_2, \tilde{\phi}_2) = (\mathrm{La}'_\xi(\theta_2), \mathrm{La}''_\xi(\theta_2) - \theta_2 \mathrm{La}_\xi(\theta_2))$ and $(w_2, \tilde{\phi}_2) = (\mathrm{Lc}'_\xi(\theta_2), \mathrm{Lc}''_\xi(\theta_2) - \theta_2 \mathrm{Lc}_\xi(\theta_2))$, respectively. We therefore introduce the following 1D solution spaces of (57):

$$
\begin{aligned}
C_{e,2} &\equiv \mathrm{span}\,\{(\tilde{y}, w_2, \tilde{\phi}_2) = (\mathrm{La}_\xi(\theta_2), \mathrm{La}'_\xi(\theta_2), \mathrm{La}''_\xi(\theta_2) - \theta_2 \mathrm{La}_\xi(\theta_2))\},\\
C_{r,2} &\equiv \mathrm{span}\,\{(\tilde{y}, w_2, \tilde{\phi}_2) = (\mathrm{Lc}_\xi(\theta_2), \mathrm{Lc}'_\xi(\theta_2), \mathrm{Lc}''_\xi(\theta_2) - \theta_2 \mathrm{Lc}_\xi(\theta_2))\}.
\end{aligned} \tag{69}
$$

We can take $C_{r,2} = \kappa_{23}(C_{r,3})$ for $\theta_2 \gg 1$ due to the algebraic decay (65) of $\mathrm{Lc}_\xi(\theta_2)$ for $\theta_2 \to \infty$. Recall that $C_{r,3}$ is nonunique as a saddle-type center manifold. We then have the following.

Proposition 15. *The space $C_{e,2}$ is transverse to $W^s(C_{r,2})$ along l_2: $(\tilde{y}, w_2, \tilde{\phi}_2)(\theta_2) \equiv 0$.*

Proof. By the exponential growth of La_ξ (see (63)) for $\theta_2 \to \infty$ it follows that the tangent space of $C_{e,2}$ is not a subspace of the tangent space of $W^s(C_{r,2})$ along l_2 for $\theta_2 \gg 1$. Hence the intersection is transverse. ∎

Returning to the variables $(y, w_2, \theta_2, \phi_2)$, $C_{e,2}$ and $C_{r,2}$ become 2D invariant manifolds of $(53)_{r_2=0}$:

$$
\begin{aligned}
C_{e,2} = \Bigg\{ &(y, w, \theta_2, \phi_2) | \theta_2 \in \mathbb{R},\ (y, w_2, \phi_2) = \left(-\frac{s}{1-\xi} + \tilde{y}, w_2, \frac{s}{1-\xi}\theta_2 + \tilde{\phi}_2 \right),\\
&(\tilde{y}, w_2, \tilde{\phi}_2) \in \mathrm{span}\,\{(\mathrm{La}_\xi(\theta_2), \mathrm{La}'_\xi(\theta_2), \mathrm{La}''_\xi(\theta_2) - \theta_2 \mathrm{La}_\xi(\theta_2))\} \Bigg\},\\
C_{r,2} = \Bigg\{ &(y, w, \theta_2, \phi_2) | \theta_2 \in \mathbb{R},\ (y, w_2, \phi_2) = \left(-\frac{s}{1-\xi} + \tilde{y}, w_2, \frac{s}{1-\xi}\theta_2 + \tilde{\phi}_2 \right),\\
&(\tilde{y}, w_2, \tilde{\phi}_2) \in \mathrm{span}\,\{(\mathrm{Lc}_\xi(\theta_2), \mathrm{Lc}'_\xi(\theta_2), \mathrm{La}''_\xi(\theta_2) - \theta_2 \mathrm{Lc}_\xi(\theta_2))^T\} \Bigg\},
\end{aligned} \tag{70}
$$

using the same symbols for the new objects in the new variables.

Lemma 16. *Consider $\theta_2 \le -\nu^{-2/3}$. Then for ν sufficiently small, the invariant manifold $C_{e,2}$ of $(53)_{r_2=0}$ can be written as a graph over (θ_2, ϕ_2),*

$$
\begin{aligned}
y &= (-\theta_2)^{-1}\phi_2 + (-\theta_2)^{-3}\left((-\theta_2)^{-1}\phi_2 + \frac{s}{1-\xi} \right) F_2((-\theta_2)^{-3}),\\
w_2 &= (-\theta_2)^{-1}(1-\xi)\left((-\theta_2)^{-1}\phi_2 + \frac{s}{1-\xi} \right)\left(1 + (-\theta_2)^{-3} G_2((-\theta_2)^{-3}) \right),
\end{aligned}
$$

where F_2 and G_2 are real analytic functions.

Proof. By (58) we find that the linear space $C_{e,2}$ in (69) is spanned by

$$\begin{aligned}
\tilde{y} &= (-\theta_2)^{-1+\xi} E_2((-\theta_2)^{-3}),\\
w_2 &= (-\theta_2)^{-2+\xi}\left((1-\xi)E_2((-\theta_2)^{-3}) + 3(-\theta_2)^{-3}E_2'((-\theta_2)^{-3})\right)\\
&\equiv (-\theta_2)^{-2+\xi}(1-\xi)\tilde{G}_2((-\theta_2)^{-3}),\\
\tilde{\phi}_2 &= (-\theta_2)^{\xi}\Bigg(E_2((-\theta_2)^{-3}) + (-\theta_2)^{-3}\Bigg((2-\xi)\left((1-\xi)E_2((-\theta_2)^{-3}) + 3(-\theta_2)^{-3}E_2'((-\theta_2)^{-3})\right)\\
&\quad + (-\theta_2)^{-3}\left((12-\xi)E_2'((-\theta_2)^{-3}) + 9(-\theta_2)^{-3}E_2''((-\theta_2)^{-3})\right)\Bigg)\Bigg)\\
&\equiv (-\theta_2)^{\xi}\tilde{H}_2((-\theta_2)^{-3}),
\end{aligned}$$

where the functions $\tilde{G}_2$ and $\tilde{H}_2$ defined by these equations are real analytic. Notice that $\tilde{H}_2(0) = E_2(0) = \Gamma(1-\xi)$. Therefore for $\theta_2 \ll 0$ we find from the last equation

$$(-\theta_2)^{\xi} = \frac{\tilde{\phi}_2}{\tilde{H}_2((-\theta_2)^{-3})}.$$

Then we substitute this expression for $(-\theta_2)^{\xi}$ into the first two equations to give

$$\begin{aligned}
\tilde{y} &= (-\theta_2)^{-1}\tilde{\phi}_2\tilde{H}_2((-\theta_2)^{-3})^{-1}E_2((-\theta_2)^{-3}),\\
w_2 &= (-\theta_2)^{-2}\tilde{\phi}_2(1-\xi)\tilde{H}_2((-\theta_2)^{-3})^{-1}\tilde{G}_2((-\theta_2)^{-3}).
\end{aligned}$$

Then the desired results follow upon returning to the original variables (using (56)) and setting

$$\begin{aligned}
F_2(u) &\equiv \int_0^1 \frac{d}{dv}\left(\tilde{H}_2(v)^{-1}E_2(v)\right)\Big|_{v=su} ds,\\
G_2(u) &\equiv \int_0^1 \frac{d}{dv}\left(\tilde{H}_2(v)^{-1}\tilde{G}_2(v)\right)\Big|_{v=su} ds.
\end{aligned}$$

■

We will continue l_2 backwards into chart κ_1 in the following section.

4.6. Entry chart κ_1.

Substituting (43) into (36) gives

$$\begin{aligned}
\dot{y} &= (1+r_1^2 f_1(r_1,\phi_1))w_1,\\
\dot{w}_1 &= \phi_1(1+r_1^2 b_1(r_1,\phi_1)) + (1+r_1^2 q_1(r_1,\phi_1))\left(-y - \delta r_1 w_1 + \varepsilon N(y, r_1 w_1, \varepsilon)\right),\\
\dot{r}_1 &= -\frac{1}{2}r_1\epsilon_1,\\
\dot{\epsilon}_1 &= \frac{3}{2}\epsilon_1^2,\\
\dot{\phi}_1 &= \epsilon_1\left(\xi(1+r_1^2 g_1(r_1,\phi_1))\left(-y - \delta r_1 w_1 + \varepsilon N(y, r_1 w_1, \varepsilon)\right) + s(1+r_1^2 h_1(r_1,\phi_1)) + \phi_1\right),
\end{aligned} \tag{71}$$

after division of the right-hand side by r_1, where $\dot{()} = \frac{d}{dt_1}$ and $\varepsilon = r_1^3\epsilon_1$. Then $\{r_1 = 0\}$ and $\{\epsilon_1 = 0\}$ are invariant subspaces. Within $\{r_1 = \epsilon_1 = 0\}$ we obtain

$$\begin{aligned}
\dot{y} &= w_1,\\
\dot{w}_1 &= \phi_1 - y,\\
\dot{\phi}_1 &= 0.
\end{aligned} \tag{72}$$

Therefore the space $\{r_1 = \epsilon_1 = 0\}$ is foliated by invariant cylinders:

$$(y - \phi_1)^2 + w_1^2 = R_0^2,\ \phi_1 < 0,\ R_0 \geq 0.$$

Each slice $\phi_1 = \text{const.} < 0$ of such a cylinder is a periodic orbit:

$$y(t_1) = \phi_1 + R_0 \cos(t_1), \quad w_1(t_1) = -R_0 \sin(t_1), \quad \phi_1(t_1) = \text{const.}$$

for (72). For $R_0 = 0$ we have

$$L_1 : y = \phi_1,\ w_1 = 0,\ \epsilon_1 = 0,\ r_1 = 0,\ \phi_1 < 0, \tag{73}$$

as a line of equilibria.

The line L_1 is normally elliptic rather than hyperbolic. This is not a surprise. In fact, we can deduce this directly from the expression (35) for the eigenvalues $\lambda_\pm$ of the layer problem (31), as follows. From (35), we have

$$\lambda_\pm = \frac{1}{2}\theta\delta \pm \sqrt{\theta} = \frac{1}{2}\theta\delta \pm i\sqrt{-\theta},$$

in terms of our new variables, ignoring for simplicity the higher order terms in $\theta \sim 0$. Setting $\theta = -r_1^2$, from (43), gives

$$\lambda_\pm = -\frac{1}{2}r_1^2\delta \pm ir_1.$$

The desingularization amplifies this eigenvalue to $\mathcal{O}(1)$ through the division of r_1 such that

$$\lambda_{1,\pm} = -\frac{1}{2}r_1\delta \pm i, \tag{74}$$

which for $r_1 = 0$ collapse to the eigenvalues $\lambda_{1,\pm} = \pm i$ we obtain by linearizing (72) about L_1.

Within $\{\epsilon_1 = 0\}$ we rediscover

$$S_{a,1} = \kappa_1(S_a) : y = \frac{1 + r_1^2 b_1(r_1, \phi_1)}{1 + r_1^2 q_1(r_1, \phi_1)}\phi_1, \quad w_1 = 0, \quad \epsilon_1 = 0, \tag{75}$$

as a manifold of equilibria. The linearization of a point in $S_{a,1}$ gives (74) (to first order in r_1) as nontrivial eigenvalues. It is attracting for $r_1 > 0$ but for $r_1 = 0$ (where $S_{a,1} \subset \{\epsilon_1 = 0\}$ collapses to L_1) it is only normally elliptic.

Similarly, by the analysis in chart κ_2, we have, within $\{r_1 = 0\}$, an invariant manifold $C_{e,1} = \kappa_{1,2}(C_{e,2})$ (recall (70)). Let

$$V_1 = \{(y, r_1, (w_1, \phi_1, \epsilon_1)) \in (-\infty, 0] \times [0, \nu] \times U_1\}$$

with U_1 as in (46).

Lemma 17. *For $\nu > 0$ sufficiently small, $C_{e,1}$ becomes*

$$\begin{aligned} y &= \phi_1 + \epsilon_1^2 \left(\phi_1 + \frac{s}{1-\xi}\right) F_2(\epsilon_1^2), \\ w_1 &= \epsilon_1(1-\xi)\left(\phi_1 + \frac{s}{1-\xi}\right)\left(1 + \epsilon_1^2 G_2(\epsilon_1^2)\right), \\ r_1 &= 0 \end{aligned}$$

within V_1, where $\epsilon_1 \in [0, \nu]$, $\phi_1 \in [-\varpi^{-1}, -\varpi]$.

Proof. This follows from Lemma 16 and the coordinate changes $\kappa_{21} = \kappa_{12}^{-1}$ and κ_{12}; see (49). ∎

Consider $r_1 = 0$ and the reduced system on $C_{e,1}$ within V_1. This gives

$$\begin{aligned} \dot{\epsilon}_1 &= \frac{3}{2}\epsilon_1, \\ \dot{\phi}_1 &= ((1-\xi)\phi_1 + s)\,(1 + \mathcal{O}(\epsilon_1)), \end{aligned} \tag{76}$$

after division of the right-hand side by ϵ_1. Here $l_1 : \epsilon_1 \geq 0$, $\phi_1 = -(1-\xi)^{-1}s$ becomes a strong unstable manifold of the unstable node $(\epsilon_1, \phi_1) = (0, -(1-\xi)^{-1}s)$ within $C_{e,1} \subset \{r_1 = 0\}$.

Lemma 18. *Let $(\tilde{y}_0, \tilde{w}_0)$ be defined as*

$$\begin{aligned} y &= \frac{1 + r_1^2 b_1(r_1, \phi_1)}{1 + r_1^2 q_1(r_1, \phi_1)}\phi_1 + \epsilon_1^2 \left(\phi_1 + \frac{s}{1-\xi}\right) F_2(\epsilon_1^2) + \tilde{y}_0, \\ w_1 &= \epsilon_1(1-\xi)\left(\phi_1 + \frac{s}{1-\xi}\right)\left(1 + \epsilon_1^2 G_2(\epsilon_1^2)\right) + \tilde{w}_0 \end{aligned} \tag{77}$$

for $(y, r_1, w_1, \phi_1, \epsilon_1) \in V_1$. Then $S_{a,1} \subset \{\epsilon_1 = 0\}$ and $C_{e,1} \subset \{r_1 = 0\}$ become

$$\begin{aligned} S_{a,1} :&\quad \tilde{y}_0 = 0, \quad \tilde{w}_0 = 0, \quad \epsilon_1 = 0, \\ C_{e,1} :&\quad \tilde{y}_0 = 0, \quad \tilde{w}_0 = 0, \quad r_1 = 0 \end{aligned}$$

within $\tilde{V}_1$: the image of V_1 under the diffeomorphism $(y, r_1, w_1, \phi_1, \epsilon_1) \mapsto (\tilde{y}_0, r_1, \tilde{w}_0, \phi_1, \epsilon_1)$ defined by (77).

Proof. Follows from (75) and Lemma 17. ∎

The main result of this section is then as follows.

Proposition 19. *Let $\nu > 0$ be sufficiently small. Then for $0 < \varepsilon \ll 1$ the forward flow of $S_{a,\varepsilon}$ intersects the $\{\epsilon_1 = \nu\}$-face of $\tilde{V}_1$ in a C^1-graph over $\phi_1 \in [-\varpi^{-1}, -\varpi]$:*

$$(\tilde{y}_0, \tilde{w}_0) = m_\varepsilon(\phi_1), \quad \phi_1 \in [-\varpi^{-1}, -\varpi]$$

with $r_1 = (\varepsilon\nu^{-1})^{1/3}$ and

$$m_\varepsilon(\phi_1) = o(1), \quad \partial_{\phi_1} m_\varepsilon(\phi_1) = o(1).$$

Proof. Full details of the proof are given in Appendix B. We present an outline here. We work with the coordinates $(\tilde{y}_0, \tilde{w}_0)$ and amplify the dissipation in (74) by a further (polar) blowup transformation (of $r_1 = \epsilon_1 = 0$) and further desingularization. However, we cannot apply blowup and desingularization directly due to the fast oscillatory part (recall, e.g., $(74)_{r_1=0}$). Therefore we first apply normal form transformations (like higher order averaging) in section B.1 to factor out this oscillatory part. The result is described in Proposition 21. Then in section B.2 we apply a van der Pol transformation (like moving into a rotating coordinate frame), given by (94). This gives rise to system (96) for which the transformed normally elliptic line L_1 (73) can be studied using a second blowup and subsequent desingularization; see (98) and section B.3. Within the chart (99), the desingularization corresponds to division by r_1 of the real part of the eigenvalues of (74) to $-\frac{1}{2}\delta$ (to leading order). Hereby we gain hyperbolicity for $r_1 = 0$ which allow us (with some technical difficulties due to the oscillatory remainder of the normal form) to extend the slow manifold $S_{a,\varepsilon}$ as a perturbation of S_a up until

$$\theta = -(\varepsilon\nu^{-1})^{1/2} \tag{78}$$

for ν sufficiently small; see Proposition 23, proved in Appendix C. We extend this further up until

$$\theta = -(\varepsilon\nu^{-1})^{2/3}, \tag{79}$$

where $\theta_2 = -\nu^{-2/3}$ and therefore $\epsilon_1 = \nu$ (cf. (49)), by applying the forward flow near a hyperbolic saddle in a subsequent chart (100) in Section B.5. The result then shows that $S_{a,\varepsilon}$ is $o(1)$-close to the invariant manifold $C_{e,1} = \kappa_{12}(C_{e,2})$ (69) of nonoscillatory solutions at the section defined by (79); see Proposition 25, which working backward then implies Proposition 19. ∎

4.7. Combining the results to prove Theorem 6. The existence of a maximal canard γ^s_ε, connecting the Fenichel slow manifold $S_{a,\varepsilon}$ with the stable manifold of $M_{r,3}(\varepsilon)$, the extension of $S_{r,\varepsilon}$ into chart κ_3, follows from Propositions 19 and 15. Indeed, Proposition 19 implies, by Lemma 18, the $o(1)$-closeness of the forward flow of $S_{a,\varepsilon}$ to $C_{e,2}$ along the $\{\theta_2 = -\nu^{-2/3}\}$-face of the box U_2 (recall Lemma 9). To finish the proof, we can therefore work in U_2 in chart κ_2 only and follow $S_{a,\varepsilon}$ from $\theta_2 = -\nu^{-2/3}$ up to $\theta_2 = \nu^{-2/3}$ using $C_{e,2}$ as a guide. By regular perturbation theory, $S_{a,\varepsilon}$ is $o(1)$-close to $C_{e,2}$ along the $\{\theta_2 = \nu^{-2/3}\}$-face of U_2. Here we also know from Proposition 10, in particular (51), that $M_{r,2}(\varepsilon) = \kappa_{23}(M_{r,3}(\varepsilon))$ is $\mathcal{O}(\varepsilon^{1/3})$-close to $C_{r,2}$. Now, combining this with Proposition 15, which states that $C_{e,2}$ intersects $W^s(C_{r,2})$ transversally along l_2, we finally conclude that the forward flow of $S_{a,\varepsilon}$ intersects $W^s(M_{r,2}(\varepsilon))$ transversally at $\theta_2 = \nu^{-2/3}$ for all $0 < \varepsilon \ll 1$. The intersection of these objects defines γ^s_ε and it follows that it is $o(1)$-close to l_2 in chart κ_2. Therefore also $\gamma^s_\varepsilon \to \gamma^s$ as $\varepsilon \to 0$.

5. Discussion and conclusions.

We have considered the problem of a slender rod slipping along a rough surface, as shown in Figure 1. In a series of classical papers, Painlevé [45, 46, 47] showed that the governing rigid body equations for this problem can exhibit multiple solutions

(the *indeterminate* case) or no solutions at all (the *inconsistent* case), provided the coefficient of friction μ exceeds a certain critical value μ_P, given by (11). Subsequently Génot and Brogliato [19] proved that, from a consistent state, the rod cannot reach an inconsistent state through slipping. Instead the rod will either stop slipping and stick or it will lift off from the surface. Between these two cases is a special solution for $\mu > \mu_C > \mu_P$, where μ_C a new critical value of the coefficient of friction, given by (16). Physically, the special solution corresponds to the rod slipping until it reaches a singular "0/0" point P, shown in Figure 2. Even though the rigid body equations cannot describe what happens to the rod beyond the singular point P, it is possible to extend the special solution into the region of indeterminacy. Hence this extended solution is very reminiscent of a *canard* [1]. To overcome the inadequacy of the rigid body equations beyond P, the rigid body assumption can be relaxed in the neighborhood of the point of contact of the rod with the rough surface. Physically this corresponds to assuming a small compliance there. So it is natural to ask what happens to both the point P and the special solution under this regularization.

In this paper, we have rigorously proved the existence of a strong canard in the *regularization by compliance* of the classical Painlevé problem. The canard is called strong because it is tangent to a strong eigendirection that appears in the rigid body formulation of Painlevé's problem. Our analysis is based on the blowup method, in the formalism developed and popularized by Krupa and Szmolyan [28, 29, 30]. Initially blowup gains us ellipticity only (rather than hyperbolicity) in the entry chart κ_1, as shown in section 4.6. As a consequence we cannot extend Fenichel's slow manifold into the scaling chart, where $\theta = \mathcal{O}(\varepsilon^{2/3})$, as a perturbation of the critical one, as is done in $(2+1)$-slow-fast systems, for example. Instead we apply a sequence of normal form transformations, followed by an additional blowup that captures the contraction in the entry chart, enabling an accurate continuation of the slow manifold up until $\theta = \mathcal{O}(\varepsilon^{1/2})$. Recall the proof of Proposition 19. From there we extend the slow manifold up until $\theta = \mathcal{O}(\varepsilon^{2/3})$ in the scaling chart κ_2 by careful estimation of the forward flow near a hyperbolic saddle. Key to the dynamics in the scaling chart κ_2 is Langer's equation (59) and its asymptotic properties.

This work was stimulated by a seminar given to the Applied Nonlinear Mathematics group in Bristol by Alan Champneys in December 2015 and attended by SJH, who immediately saw the potential for the use of blowup in this field. The main work in this paper was carried out during the spring and autumn of 2016. Subsequently the current authors were made aware of the paper by Nordmark, Várkonyi, and Champneys [42]. That paper addresses a wider class of rigid body problems than we do here. Canards are also studied and Langer's equation also appears. These authors use formal asymptotic methods and numerical computations, rather than our GSPT and blowup approach.

One important difference between our two approaches lies in the number of different cases that are covered. We consider the class of rigid body problem where, for $\mu > \mu_C$, the weak direction is $\theta = \theta_1$ and the strong direction lies between the first and third quadrants of Figure 2. When $\mu_P < \mu < \mu_C$, the strong direction is $\theta = \theta_1$ and the weak direction lies between the second and fourth quadrants (but does not correspond to a weak canard). Thus our case corresponds to Case II of Figure 3 in Nordmark, Várkonyi, and Champneys [42].

So the question naturally arises as to whether we could extend our approach to prove the existence of weak canards in more general settings (Case III of [42]). Weak canards in

$(2+1)$-slow-fast systems are obtained as the intersection of an extension of Fenichel's slow manifold as a perturbation of the critical one into the scaling chart. The weak canards do not necessarily intersect the original Fenichel slow manifold. But then, as we are unable to extend the slow manifold into the scaling chart as a perturbation, it is therefore at this stage questionable, given the contraction toward the weak singular canard, whether one can really obtain a sensible notion of these canards for the compliant version when $0 < \varepsilon \ll 1$. It seems that the result may depend upon the contraction rate of the slow-flow toward the weak singular canard.

Appendix A. Proof of Lemma 13: Properties of the solutions of Langer's equation.

In section 4.5, we considered *Langer*'s [33, 34] third order linear ODE:

$$y'''(\theta) = \theta y'(\theta) + (1-\xi)y(\theta) \tag{80}$$

with $\xi \in (0,1)$, where in this appendix, we drop both the subscripts and tildes in comparison with (59). The computations and analysis we perform in this section follow similar arguments used for studying the solutions of the Airy equation

$$A''(\theta) = \theta A(\theta). \tag{81}$$

In fact, (80) is related to the Airy equation; see [54]. For $\xi = 0$ we obtain (80) from $(81)_{A=y}$ by differentiating with respect to θ. For $\xi = 1$, we obtain (81) by setting $A = y'$. For the case when ξ is a relative integer $1/n$, $n \in \mathbb{N}$, the solution involves algebraic combinations of Airy functions Ai and Bi, their integrals, and their derivatives (see [53, 54]). In particular, for $\xi = \frac{1}{2}$, it is a straigthforward calculation to show that $y = A(2^{-2/3}\theta)^2$ solves (80) when A solves (81). The solution for $\xi = \frac{1}{2}$ is therefore a linear combination of $\mathrm{Ai}(2^{-2/3}\theta)^2$, $\mathrm{Bi}(2^{-2/3}\theta)^2$, and $\mathrm{Ai}(2^{-2/3}\theta)\mathrm{Bi}(2^{-2/3}\theta)$.

To proceed for general $\xi \in (0,1)$, we consider the solution ansatz

$$y(\theta) = \int_\Upsilon \hat{y}(z) e^{\theta z} dz,$$

following Laplace, where both the complex analytic function $\hat{y}(z)$, $z = u + iv \in D \subset \mathbb{C}$, and the unbounded contour $\Upsilon \subset D$ are to be determined. Suppose that $\hat{y}|_{\partial\Upsilon} = 0$ and that the integral and its first three derivatives with respect to u converge absolutely. Then insertion into (80) gives

$$\int_\Upsilon \left(z^3\hat{y}(z) + z\hat{y}'(z) + \xi\hat{y}(z)\right) e^{\theta z} dz = 0,$$

upon using integration by parts. Therefore we set

$$\hat{y}(z) = e^{-z^3/3 - \xi \log z} \tag{82}$$

with $z \neq 0$ as a solution of

$$z^3\hat{y}(z) + z\hat{y}'(z) + \xi\hat{y}(z) = 0.$$

This gives rise to the following solution of (80):

$$y(\theta) = \int_{\Upsilon} e^{-z^3/3+\theta z} e^{-\xi \log z} dz \tag{83}$$

for appropriately chosen contours Υ. Given that $\hat{y}|_{\partial\Upsilon} = 0$ we restrict attention to those z that asymptotically satisfy $\mathrm{Re}\,(z^3) < 0$, or equivalently

$$\mathrm{Arg}_\pi(z) \in (-\pi/6, \pi/6) \cup (\pi/2, 5\pi/6) \cup (-5\pi/6, -\pi/2) \tag{84}$$

for $|z| \gg 0$. Here $\mathrm{Arg}_\pi \in (-\pi, \pi)$ is the principal value argument of z. We will later also need the separate argument

$$\mathrm{Arg}_0(z) \in (0, 2\pi) \tag{85}$$

of $z \in \mathbb{C}$. The "ends" of the contour Υ should asymptotically be confined to the set in (84). Furthermore, $0 \notin \Upsilon$. But note that, since $\xi \in (0, 1)$, the function $z^{-\xi}$ is integrable over $z \in (0, a)$ with $a > 0$.

To obtain the three different linearly independent solutions La_ξ, Lb_ξ, and Lc_ξ in Lemma 13 we consider three different paths Υ_1, Υ_2, and Υ_3 together with two different branch cuts for the complex logarithm appearing in (82).

Appendix A is organized as follows. The three solutions La_ξ, Lb_ξ, and Lc_ξ are considered in sections A.1, A.2, and A.3, respectively. Then their asymptotics for $\theta \to \infty$ are considered in sections A.4, A.5, and A.6, respectively, and for $\theta \to -\infty$, in sections A.7, A.8, and A.9, respectively.

A.1. Solution La_ξ. We will obtain the solution La_ξ by considering the integral (83) over the contour $\Upsilon_{1,\nu}$, shown in Figure 3(a) and defined as

$$\Upsilon_{1,\nu} = \Upsilon^-_{1,\nu} \cup \Upsilon^+_{1,\nu} \cup \Upsilon^0_{1,\nu},$$

where

$$\begin{aligned}
\Upsilon^-_{1,\nu} &= \{z \in \mathbb{C} | \mathrm{Im}(z) = -\nu,\ \mathrm{Re}(z) \geq 0\},\\
\Upsilon^0_{1,\nu} &= \{z \in \mathbb{C} | |z| = \nu,\ \mathrm{Re}(z) < 0\},\\
\Upsilon^+_{1,\nu} &= \{z \in \mathbb{C} | \mathrm{Im}(z) = +\nu,\ \mathrm{Re}(z) \geq 0\}
\end{aligned}$$

for $\nu > 0$. The path of integration is clockwise. We take a branch cut along $\arg(z) = 0$ and define the complex logarithm in (82) as

$$\log_0(z) \equiv \ln|z| + i\mathrm{Arg}_0(z), \tag{86}$$

where Arg_0 is the argument in (85). To ensure that La_ξ is real we multiply (83) by $(1 - e^{-\xi 2\pi i})^{-1}$ and therefore set

$$\mathrm{La}_\xi(\theta) = (1 - e^{-\xi 2\pi i})^{-1} \int_{\Upsilon_{1,\nu}} e^{-z^3/3+\theta z} e^{-\xi \log_0(z)} dz.$$

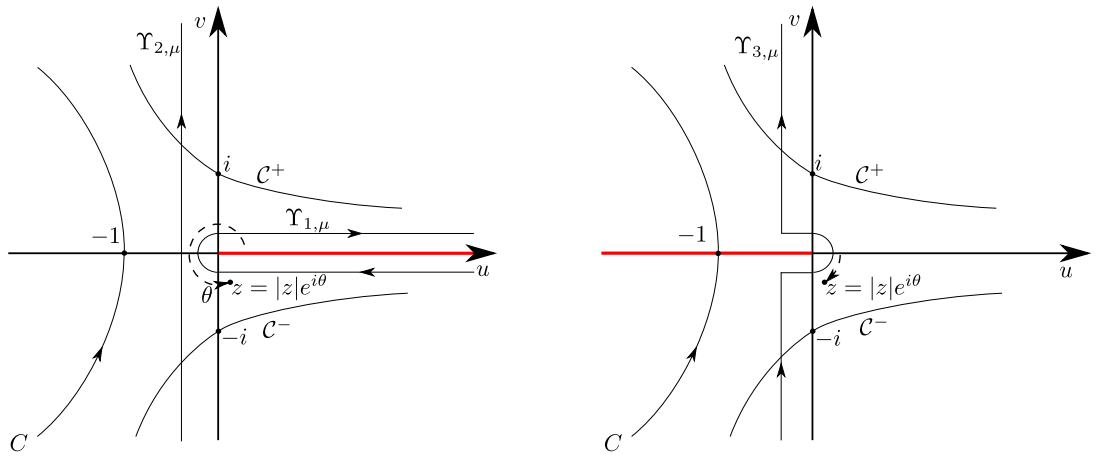

Figure 3. (a) *Illustration of the contours* $\Upsilon_{1,\nu}$ *and* $\Upsilon_{2,\nu}$. *To determine the asymptotics of* Lb_ξ *we will use the contours* C *and* $\mathcal{C}^\pm$. (b) *Illustration of the contour* $\Upsilon_{3,\nu}$. *To determine the asymptotics of* Lc_ξ *we will use the contours* C *and* $\mathcal{C}^\pm$.

Since $\xi \in (0,1)$ and the integrand is analytic away from $\arg(z)=0$, we easily conclude that

$$\begin{aligned}\mathrm{La}_\xi(\theta) &= (1-e^{-\xi 2\pi i})^{-1}\left(\int_\infty^0 e^{-\tau^3/3+\theta\tau}e^{-\xi(\ln\tau+i2\pi)}d\tau + \int_0^\infty e^{-\tau^3/3+\theta\tau}e^{-\xi\ln\tau}d\tau\right)\\ &= \int_0^\infty e^{-\tau^3/3+\theta\tau}\tau^{-\xi}d\tau, \qquad (87)\end{aligned}$$

upon sending $\nu \to 0^+$, in agreement with (60).

A.2. Solution Lb_ξ. The solution Lb_ξ is obtained by considering the integral (83) over a contour $\Upsilon_{2,\nu}$, shown in Figure 3(a) and defined as

$$\Upsilon_{2,\nu} = \{z \in \mathbb{C} | \mathrm{Re}(z) = -\nu\}.$$

The direction of integration is along positive $\mathrm{Im}(z)$. Furthermore, we take a branch cut along $\arg(z)=0$ and define the complex logarithm in (82) as in (86). To ensure that Lb_ξ is real, we multiply (83) by $\frac{1}{2i}e^{i\xi\pi}$ and therefore set

$$\mathrm{Lb}_\xi(\theta) = \frac{1}{2i}e^{i\xi\pi}\int_{\Upsilon_{2,\nu}} e^{-z^3/3+\theta z}e^{-\xi\log_0(z)}dz. \qquad (88)$$

Again, since $\xi \in (0,1)$ and the integrand is analytic away from $\arg(z)=\pi$, we easily conclude that

$$\mathrm{Lb}_\xi(\theta) = \int_0^\infty \cos(\tau^3/3+\theta\tau+\xi\pi/2)\tau^{-\xi}d\tau,$$

upon sending $\nu \to 0^+$, in agreement with (61).

Remark 20. Note that the expressions for Lb_ξ with $\xi = 0$ and $\xi = 1$ collapse to

$$\mathrm{Lb}_\xi(\theta) = \int_0^\infty \cos(\tau^3/3 + \theta\tau)d\tau = \pi \mathrm{Ai}\,(\theta)$$

and

$$\mathrm{Lb}_\xi(\theta) = \int_0^\infty \cos(\tau^3/3 + \theta\tau + \pi/2)\tau^{-1}d\tau = \int_0^\infty -\sin(\tau^3/3 + \theta\tau)\tau^{-1}d\tau = -\pi\int_0^\theta \mathrm{Ai}\,(u)du - \frac{\pi}{6},$$

respectively. For $\xi = 1$ we have used that $\int_0^\infty \sin(\tau^3/3)\tau^{-1}d\tau = \frac{\pi}{6}$.

A.3. Solution Lc_ξ. For the solution Lc_ξ we select the contour $\Upsilon_{3,\nu}$, shown in Figure 3(b) and defined as

$$\Upsilon_{3,\nu} = \Upsilon^-_{3,\nu} \cup \Upsilon^+_{3,\nu} \cup \Upsilon^0_{3,\nu},$$

where

$$\begin{aligned}
\Upsilon^-_{3,\nu} &= \{z \in \mathbb{C} | \mathrm{Re}(z) = -\nu,\ \mathrm{Im}(z) \geq \nu\},\\
\Upsilon^0_{3,\nu} &= \{z \in \mathbb{C} | \mathrm{Im}(z) = \pm\nu,\ \mathrm{Re}(z) \in (-\nu, 0)\} \cup \{z \in \mathbb{C} | |z| = \nu,\ \mathrm{Re}(z) \geq 0\},\\
\Upsilon^+_{3,\nu} &= \{z \in \mathbb{C} | \mathrm{Re}(z) = -\nu,\ \mathrm{Im}(z) \leq -\nu\}
\end{aligned}$$

for $\nu > 0$. The integration is anticlockwise. Furthermore, we take a branch cut along $\arg(z) = \pi$ and define the complex logarithm in (82) as

$$\log_\pi(z) \equiv \ln|z| + i\mathrm{Arg}_\pi(z).$$

To ensure that Lc_ξ is real we multiply (83) by $\frac{1}{2i}$ and therefore set

$$\mathrm{Lc}_\xi(\theta) = \frac{1}{2i}\int_{\Upsilon_{3,\nu}} e^{-z^3/3+\theta z}e^{-\xi\log_\pi(z)}dz,$$

which as above gives

$$\mathrm{Lc}_\xi(\theta) = \int_0^\infty \cos(\tau^3/3 + \theta\tau - \xi\pi/2)\tau^{-\xi}d\tau,$$

upon sending $\nu \to 0^+$, in agreement with (62).

Now we describe the asymptotics of each of the functions La_ξ, Lb_ξ, and Lc_ξ as $\theta \to \pm\infty$.

A.4. Asymptotics of La_ξ for $\theta \to \infty$. To study the behavior of the function La_ξ in the limit $\theta \to \infty$, we consider (87) and set $\tau = \sqrt{\theta}s$ so that

$$\begin{aligned}
\mathrm{La}_\xi(\theta) &= \theta^{(1-\xi)/2}\int_0^\infty e^{\theta^{3/2}(-s^3/3+s)}s^{-\xi}ds\\
&= \theta^{(1-\xi)/2}e^{2\theta^{3/2}/3}\int_{-1}^\infty e^{\theta^{3/2}(-s^2(1+s/3))}(1+s)^{-\xi}ds
\end{aligned}$$

and then using the fact that $\frac{1}{\sqrt{\pi}a}e^{-1/a^2s^2}$ is a δ-sequence as $a \equiv \theta^{-3/4} \to 0$ we obtain

$$\mathrm{La}_\xi(\theta) = \sqrt{\pi}\theta^{(1-\xi)/2-3/4}e^{2\theta^{3/2}/3}(1 + o(1))$$

as $\theta \to \infty$, in agreement with (63).

A.5. Asymptotics of Lb_ξ for $\theta \to \infty$. To compute the asymptotics of Lb_ξ in (88) for $\theta \to \infty$, we replace z by $\sqrt{\theta}z$ so that

$$\mathrm{Lb}_\xi(\theta) = \frac{1}{2i} e^{i\xi\pi} \theta^{(1-\xi)/2} \int_{\Upsilon_{2,\nu}} e^{\theta^{3/2} F(z)} e^{-\xi \log_0 z} dz, \tag{89}$$

where

$$F(z) = -z^3/3 + z.$$

In (89) we have used the fact that the integrand is analytic away from $\arg(z) = 0$ to replace the path of integration $\Upsilon_{2,\nu}/\sqrt{\theta}$ by $\Upsilon_{2,\nu}$. Then we follow standard arguments used for computing the asymptotics of the Airy function Ai, deforming $\Upsilon_{2,\nu}$ into

$$C = \{z = u + iv \in \mathbb{C} | u = q(v^2)\}, \tag{90}$$

where

$$q(v^2) \equiv -\sqrt{v^2/3 + 1}.$$

Along C we have $\operatorname{Im} F(z) = 0$ and

$$\operatorname{Re} F(z) = -\frac{2}{3}\sqrt{v^2/3+1}\left(1 + \frac{4}{3}v^2\right) = -\frac{2}{3} - v^2(1 + \mathcal{O}(v^2)).$$

Using again that $\frac{1}{\sqrt{\pi}a} e^{-1/a^2 s^2}$ is a δ-sequence as $a \equiv \theta^{-3/4} \to 0$ we obtain

$$\mathrm{Lb}_\xi(\theta) = \frac{1}{2i} e^{i\xi\pi} \theta^{(1-\xi)/2} \int_C e^{\theta^{3/2} F(z)} e^{-\xi \log_0 z} dz = \frac{\sqrt{\pi}}{2} \theta^{(1-\xi)/2 - 3/4} e^{-2\theta^{3/2}/3} (1 + o(1))$$

for $\theta \to \infty$, in agreement with (64).

A.6. Asymptotics of Lc_ξ for $\theta \to \infty$. To compute the asymptotics of Lc_ξ for $\theta \to \infty$, we proceed as for Lb_ξ. We replace z by $\sqrt{\theta}z$ and then use the analyticity of the integrand away from $\arg(z) = \pi$ to deform $\Upsilon_{3,\nu}$ into a union of $C \cap \{\mathrm{Im}(z) \gtrless \pm\nu\}$ with C as in (90) and

$$\tilde{\Upsilon}^0_{3,\nu} = \{z \in \mathbb{C} | \mathrm{Im}(z) = \pm\nu,\ \mathrm{Re}(z) \in (-q(\nu^2), 0)\} \cup \{z \in \mathbb{C} | |z| = \nu,\ \mathrm{Re}(z) \geq 0\}.$$

The contribution from $C \cap \{\mathrm{Im}(z) \gtrless \pm\nu\}$ is exponentially small $\mathcal{O}(e^{-2/3\theta^{3/2}})$ as $\theta \to \infty$. Therefore

$$\begin{aligned}\mathrm{Lc}_\xi(\theta) &= \frac{1}{2i} \theta^{(1-\xi)/2} \int_{\tilde{\Upsilon}^0_{3,\nu}} e^{\theta^{3/2}(-z^3/3+z)} e^{-\xi \log_\pi(z)} dz + \mathcal{O}(e^{-2/3\theta^{3/2}}) \\ &= \sin(\xi\pi) \theta^{(1-\xi)/2} \int_0^1 e^{\theta^{3/2}(\tau^3/3-\tau)} \tau^{-\xi} d\tau + \mathcal{O}(e^{-2/3\theta^{3/2}}),\end{aligned}$$

upon $\nu \to 0^+$. The function

$$G(\nu) = \nu^{\xi-1} \int_0^1 e^{\nu^{-1}(\tau^3/3-\tau)} \tau^{-\xi} d\tau = \int_0^{\nu^{-1}} e^{-s+\nu^2 s^3/3} s^{-\xi} ds$$

is continuous at $\nu = 0$ with value

$$G(0) = \int_0^1 e^{-w} w^{-\xi} dw = \Upsilon(1-\xi),$$

where Υ on the right-hand side is for the Υ-function. Therefore

$$\mathrm{Lc}_\xi(\theta) = \sin(\xi\pi)\theta^{(1-\xi)/2-3/2}\Upsilon(1-\xi)(1+o(1)),$$

in agreement with (65).

A.7. Asymptotics of La_ξ for $\theta \to -\infty$. First we replace τ by $(-\theta)^{1/2}\tau$ and obtain

$$\mathrm{La}_\xi(\theta) = (-\theta)^{(1-\xi)/2} \int_0^\infty e^{(-\theta)^{3/2}(-\tau^3-\tau)} \tau^{-\xi} d\tau.$$

Then we apply the following substitution

$$t(\tau) = \tau^3/3 + \tau$$

with inverse

$$\tau = t(1 + m(t^2))$$

with m real analytic. Then

$$\mathrm{La}_\xi(\theta) = (-\theta)^{(1-\xi)/2} \int_0^\infty e^{-(-\theta)^{3/2}t} t^{-\xi}(1+n(t^2))dt,$$

where $n = (1+m)^{-\xi}\frac{d\tau}{dt} - 1$ is real analytic with $n(0) = 0$. Finally, setting $s = (-\theta)^{3/2}t$ gives

$$\mathrm{La}_\xi(\theta) = (-\theta)^{-(1-\xi)} E_2((-\theta)^{-3})$$

with

$$E_2(w) = \int_0^\infty e^{-s} s^{-\xi}(1+n(ws^2))ds,$$

a real-analytic function, in agreement with (66).

A.8. Asymptotics of Lb_ξ for $\theta \to -\infty$. The asymptotics of Lb_ξ for $\theta \to -\infty$ is obtained by replacing z by $(-\theta)^{1/2}z$. This gives

$$\mathrm{Lb}_\xi(\theta) = \frac{1}{2i} e^{i\xi\pi} (-\theta)^{(1-\xi)/2} \int_{\Upsilon_{2,\nu}} e^{(-\theta)^{3/2}G(z)} e^{-\xi \log_0(z)} dz,$$

where

$$G(z) = -z^3/3 - z.$$

We then replace the contour $\Upsilon_{2,\nu}$ with a union of $\Upsilon_{1,\nu}$ and

$$\mathcal{C}^+ = \{z = u + iv \in \mathbb{C} | u = s_+(v),\ v > 0\},$$
$$\mathcal{C}^- = \{z = u + iv \in \mathbb{C} | u = s_-(v),\ v < 0\},$$

where

$$s_\pm(v) = \pm(v \mp 1)\sqrt{\frac{v \pm 2}{3v}}.$$

The contours $\mathcal{C}^\pm$ are also used to study the asymptotics of the Airy function $\mathrm{Ai}(\theta)$ for $\theta \to -\infty$. Along $\mathcal{C}^\pm$ we have $\mathrm{Im}(G) = \mp\frac{2}{3}$ and

$$\mathrm{Re}(G) = s_\pm(v)\left(-s_\pm(v)^2/3 + v^2 - 1\right) = 2(v \mp 1)^2(1 + \mathcal{O}(v \mp 1)).$$

In particular, $\mathrm{Re}(G)$ has a global maximum along $\mathcal{C}^\pm$ at $v = \pm 1$, respectively. This then leads to

$$\begin{aligned}\mathrm{Lb}_\xi(\theta) &= \frac{1}{2i}e^{i\xi\pi}(-\theta)^{(1-\xi)/2}\int_{\mathcal{C}^+\cup\mathcal{C}^-} e^{(-\theta)^{3/2}G(z)}e^{-\xi\log_0(z)}dz + \frac{1}{2i}e^{i\xi\pi}(1 - e^{-\xi 2\pi i})\mathrm{La}_\xi(\theta)\\ &= \sqrt{2\pi}(-\theta)^{(1-\xi)/2-3/4}\sin\left(\frac{2}{3}(-\theta)^{3/2}(1 + o(1)) + \frac{\pi}{4} - \frac{\xi\pi}{2}\right)(1 + o(1))\\ &\quad + \sin(\xi\pi)\mathrm{La}_\xi(\theta),\end{aligned}$$

in agreement with (67).

A.9. Asymptotics of Lc_ξ for $\theta \to -\infty$. In this case we replace z by $(-\theta)^{1/2}z$ and deform $\Upsilon_{3,\nu}$ into $\mathcal{C}^+ \cup \mathcal{C}^-$. The calculations are similar to the asymptotics of Lb_ξ as $\theta \to -\infty$. We obtain

$$\mathrm{Lc}_\xi(\theta) = \sqrt{2\pi}(-\theta)^{(1-\xi)/2-3/4}\sin\left(\frac{2}{3}(-\theta)^{3/2}(1 + o(1)) + \frac{\pi}{4} + \frac{\xi\pi}{2}\right)(1 + o(1)),$$

in agreement with (68).

Appendix B. Proof of Proposition 19.

From (71) in section 4.6, we obtain the following equations in terms of the $(\tilde{y}_0, \tilde{w}_0)$-variables defined by (77):

(91)

$$\begin{aligned}\dot{\tilde{y}}_0 &= \epsilon_1\xi\left(1 + Q_1^{(0)}(\tilde{y}_0, \tilde{w}_0, r_1, \phi_1, \epsilon_1)\right)\tilde{y}_0 + \left(1 + Q_2^{(0)}(r_1, \phi_1, \epsilon_1)\right)\tilde{w}_0 + r_1\epsilon_1 Q_0^{(0)}(r_1, \phi_1, \epsilon_1),\\ \dot{\tilde{w}}_0 &= \left(-1 + P_2^{(0)}(r_1, \phi_1, \epsilon_1)\right)\tilde{y}_0 + \left(-\delta r_1 + \frac{1}{2}\epsilon_1 + P_1^{(0)}(\tilde{y}_0, \tilde{w}_0, r_1, \phi_1, \epsilon_1)\right)\tilde{w}_0 + r_1\epsilon_1 P_0^{(0)}(r_1, \phi_1, \epsilon_1),\\ \dot{r}_1 &= -\frac{1}{2}r_1\epsilon_1,\\ \dot{\epsilon}_1 &= \frac{3}{2}\epsilon_1^2,\\ \dot{\phi}_1 &= \epsilon_1\left(((1 - \xi)\phi_1 + s)\left(1 - \frac{\epsilon_1^2}{1 - \xi}F_2(\epsilon_1^2)\right) + V^{(0)}(\tilde{y}_0, \tilde{w}_0, r_1, \phi_1, \epsilon_1)\right),\end{aligned}$$

the equations defining new smooth functions $Q_i^{(0)}$, $P_i^{(0)}$, $V^{(0)}$ satisfying

$$Q_1^{(0)}, Q_2^{(0)}, P_1^{(0)}, P_2^{(0)} = \mathcal{O}((\epsilon_1 + r_1)^2 + \varepsilon(\tilde{y}_0 + \tilde{w}_0)), \quad V^{(0)} = \mathcal{O}(r_1(\tilde{w}_0 + r_1 + \epsilon_1) + \tilde{y}_0).$$

Recall $\varepsilon = r_1^3\epsilon_1$. We will now consider this system in detail.

Specifically, since we cannot apply blowup and desingularization directly due to the fast oscillatory part (recall, e.g., $(74)_{r_1=0}$), we first apply normal form transformations in section B.1 to factor out this oscillatory part. These normal form transformations are like higher order averaging. But the normal form approach circumvents the singularity associated with the zero amplitude that is known to appear when using averaging in this context. Then in section B.2 we apply a van der Pol transformation (moving into a rotating coordinate frame), giving rise to (96). In section B.3 the transformed normally elliptic line L_1 (73) can be studied using a second blowup and subsequent desingularization. Within chart (99), we gain hyperbolicity for $r_1 = 0$ which allows us to extend the slow manifold $S_{a,\varepsilon}$ as a perturbation of S_a up until $\theta = -(\varepsilon\nu^{-1})^{1/2}$ for $\nu > 0$ sufficiently small but fixed with respect to $\varepsilon > 0$. We extend this further into $\theta = -(\varepsilon\nu^{-1})^{2/3}$ (where $\epsilon_1 = \nu$ cf. (49)) by applying the forward flow in a subsequent chart (100) in section B.5. We find that $S_{a,\varepsilon}$ is $o(1)$-close to the manifold $C_{e,1} = \kappa_{12}(C_{e,2})$ (69) of nonoscillatory solutions at the section defined by (79); see Proposition 25, which working backward then implies Proposition 19.

B.1. Normal form transformation.

Let

$$\tilde{V}_1 = \{(\tilde{y}, r_1, (\tilde{w}_1, \phi_1, \epsilon_1)) \in [-\sigma, \sigma] \times [0, \nu] \times \tilde{U}_1\}$$

with $\tilde{U}_1 = [-\sigma, \sigma] \times [-\varpi^{-1}, -\varpi] \times [0, \nu]$.

Proposition 21. *Fix any $n \in \mathbb{N}$. Then for $\nu > 0$ sufficiently small there exists a smooth mapping*

$$\Phi_n : \quad \tilde{V}_1 \ni (\tilde{y}_0, r_1, \tilde{w}_0, \phi_1, \epsilon_1) \mapsto (\tilde{y}_n, r_1, \tilde{w}_n, \phi_1, \epsilon_1),$$

leaving r_1, ϕ_1, ϵ_1 invariant, that transforms (91) into

$$\begin{aligned}
\dot{\tilde{y}}_n &= \left(T^{(n)}(I_n, r_1, \phi_1, \epsilon_1) + Q_1^{(n)}(\tilde{y}_n, \tilde{w}_n, r_1, \phi_1, \epsilon_1)\right)\tilde{y}_n \\
&\quad + \left(1 + \Omega^{(n)}(I_n, r_1, \phi_1, \epsilon_1) + Q_2^{(n)}(\tilde{y}_n, \tilde{w}_n, r_1, \phi_1, \epsilon_1)\right)\tilde{w}_n + r_1\epsilon_1 Q_0^{(n)}(r_1, \phi_1, \epsilon_1), \\
\dot{\tilde{w}}_n &= -\left(1 + \Omega^{(n)}(I_n, r_1, \phi_1, \epsilon_1) + P_2^{(n)}(\tilde{y}_n, \tilde{w}_n, r_1, \phi_1, \epsilon_1)\right)\tilde{y}_n \\
&\quad + \left(T^{(n)}(I_n, r_1, \phi_1, \epsilon_1) + P_1^{(n)}(\tilde{y}_n, \tilde{w}_n, r_1, \phi_1, \epsilon_1)\right)\tilde{w}_n + r_1\epsilon_1 P_0^{(n)}(r_1, \phi_1, \epsilon_1), \\
\dot{r}_1 &= -\frac{1}{2} r_1\epsilon_1, \\
\dot{\epsilon}_1 &= \frac{3}{2}\epsilon_1^2, \\
\dot{\phi}_1 &= \epsilon_1\left(((1-\xi)\phi_1 + s)\left(1 - \frac{\epsilon_1^2}{1-\xi}F_2(\epsilon_1^2)\right) + V^{(n)}(\tilde{y}_n, \tilde{w}_n, r_1, \phi_1, \epsilon_1)\right),
\end{aligned} \tag{92}$$

where

$$Q_1^{(n)}, Q_1^{(n)}, P_1^{(n)}, P_2^{(n)} = \mathcal{O}_1 + \varepsilon\mathcal{O}_2, \quad Q_0^{(n)}, P_0^{(n)} = \mathcal{O}_1, \quad V^{(n)} = \mathcal{O}_3,$$

where

$$I_n = |(\tilde{y}_n, \tilde{w}_n)|^2 = \tilde{y}_n^2 + \tilde{w}_n^2,$$

and

$$\mathcal{O}_1 = \mathcal{O}(|(r_1, \epsilon_1)|^n), \quad \mathcal{O}_2 = \mathcal{O}((\tilde{y}_n + \tilde{w}_n)|(r_1, \tilde{y}_n, \tilde{w}_n, \epsilon_1)|^{n-1}),$$
$$\mathcal{O}_3 = \mathcal{O}(r_1(\tilde{w}_n + r_1 + \epsilon_1) + \tilde{y}_n).$$

Furthermore $T^{(n)}$ and $\Omega^{(n)}$ are nth-degree polynomials of I_n, r_1, ϵ_1 with ϕ_1-dependent coefficients, satisfying

$$T^{(n)}(I_n, r_1, \phi_1, \epsilon_1) = -\frac{1}{2}\delta r_1 + \frac{1}{2}\left(\frac{1}{2} + \xi\right)\epsilon_1 + \mathcal{O}((r_1 + \epsilon_1)^2 + \varepsilon I_n), \tag{93}$$
$$\Omega^{(n)}(I_n, r_1, \phi_1, \epsilon_1) = \mathcal{O}((r_1 + \epsilon_1)^2 + \epsilon I_n).$$

Proof. The linearization about

$$(\tilde{y}_0, \tilde{w}_0, r_1, \epsilon_1, \phi_1) = (0, 0, 0, 0, -(1 - \xi)^{-1}s)$$

gives

$$L = \begin{pmatrix} L_0 & 0_{2\times 3} \\ 0_{3\times 2} & 0_{3\times 3} \end{pmatrix}, \quad L_0 = \begin{pmatrix} 0 & 1 \\ -1 & 0 \end{pmatrix}.$$

By normal form theory (see, e.g., [20, Theorem 1.2 and Lemma 1.7]), the system can be brought into (92) by successive transformations, the truncated system with $Q_i^{(n)} = P_i^{(n)} = 0$ being equivariant with respect the action of e^{tL}. Simple calculations then give (93). ∎

We shall henceforth drop the subscripts on r_1, ϕ_1, and ϵ_1.

B.2. Van der Pol transformation. Now we apply the van der Pol transformation

$$\begin{pmatrix} \tilde{y}_n \\ \tilde{w}_n \end{pmatrix}(t_1) = A(\psi(t_1))z(t_1), \quad \dot{\psi}(t_1) = 1, \tag{94}$$

to (92), where $\psi \in S^1$, $z \in \mathbb{R}^2$, and

$$A(\psi) = \begin{pmatrix} \cos\psi & \sin\psi \\ -\sin\psi & \cos\psi \end{pmatrix} \in SO(2), \tag{95}$$

to give the extended system,

$$
\begin{aligned}
\dot{z} &= \left(\begin{pmatrix} T^{(n)}(|z|^2, r, \phi, \epsilon) & \Omega^{(n)}(|z|^2, r, \phi, \epsilon) \\ -\Omega^{(n)}(|z|^2, r, \phi, \epsilon) & T^{(n)}(|z|^2, r, \phi, \epsilon) \end{pmatrix} + R^{(n)}(z, r, \phi, \epsilon, \psi) \right) z \\
&\quad + \epsilon r \mathcal{R}^{(n)}(r, \phi, \epsilon, \psi), \\
\dot{r} &= -\frac{1}{2} r \epsilon, \\
\dot{\epsilon} &= \frac{3}{2} \epsilon^2, \\
\dot{\phi} &= \epsilon \left(((1-\xi)\phi + s) \left(1 - \frac{\epsilon^2}{1-\xi} F(\epsilon^2) \right) + V^{(n)}(A(\psi) z, r, \phi, \epsilon) \right), \\
\dot{\psi} &= 1,
\end{aligned} \tag{96}
$$

on $(z, r, \phi, \epsilon, \psi) \in \mathbb{R}^5 \times S^1$ with

$$
\mathcal{R}^{(n)} = \mathcal{O}(|(r,\epsilon)|^n + r^3 \epsilon |z| |(r, z, \epsilon)|^{n-1}),\ \mathcal{R}^{(n)} = \mathcal{O}(|(r,\epsilon)|^n),\ V^{(n)} = \mathcal{O}(z + r_1(r_1 + \epsilon_1)).
$$

Recall also (93). We will work with system (96) henceforth. By construction, we have the following lemma.

Lemma 22. *System* (96) *possesses an* S^1*-symmetry:*

$$
\mathcal{S}_\nu : \quad z \mapsto A(\nu) z, \quad \psi \mapsto \psi - \nu, \tag{97}
$$

for every $\nu \in S^1$.

B.3. Subsequent blowup. Setting $\epsilon = 0$ in (96) gives $z = 0$ as a set of equilibria, corresponding to $S_{a,1}$. Therefore it is also nonnormally hyperbolic at $r = 0$. Indeed $T^{(n)}(0, 0, \phi, 0) \equiv 0$. Therefore we apply the following polar blowup transformation to (96),

$$
r = \rho \bar{r}, \quad \epsilon = \rho \bar{\epsilon}, \quad \rho \geq 0, (\bar{r}, \bar{\epsilon}) \in S^1, \tag{98}
$$

and desingularize through division of the right-hand side by ρ. The transformation (98) blows up $r = \epsilon = 0$ to a sphere $(\bar{r}, \bar{\epsilon}) \in S^1$. We consider two directional charts:

$$
\bar{r} = 1 : \quad r = \rho_1, \quad \epsilon = \rho_1 \epsilon_1, \quad \epsilon_1 \in I_1, \tag{99}
$$

and

$$
\bar{\epsilon} = 1 : \quad r = \rho_2 r_2, \quad \epsilon = \rho_2, \quad r_2 \in I_2. \tag{100}
$$

Here I_1 and I_2 are sufficiently large open sets that contain $[0, \nu]$ and $[0, \nu^{-1}]$, respectively. In this way the two charts (99) and (100) cover $(\bar{r}, \bar{\epsilon}) \in S^1$ with $\bar{\epsilon} \geq 0$, $\bar{r} \geq 0$. The coordinate changes are defined by

$$
\rho_1 = \rho_2 r_2, \quad \epsilon_1 = r_2^{-1}. \tag{101}
$$

Notice that the conservation $r^3\epsilon = \varepsilon$ in chart κ_1 becomes

$$\rho_1^4\epsilon_1 = \varepsilon, \tag{102}$$

and

$$\rho_2^4 r_2^3 = \varepsilon, \tag{103}$$

in charts (99) and (100), respectively.

B.4. Chart (99). In this chart we obtain the following set of equations from (96):

$$\begin{aligned}
\dot{z} &= \left(\begin{pmatrix} T_1^{(n)}(|z|^2,\rho_1,\phi,\epsilon_1) & \Omega_1^{(n)}(|z|^2,\rho_1,\phi,\epsilon_1) \\ -\Omega_1^{(n)}(|z|^2,\rho_1,\phi,\epsilon_1) & T_1^{(n)}(|z|^2,\rho_1,\phi,\epsilon_1) \end{pmatrix} + R_1^{(n)}(z,\rho_1,\phi,\epsilon_1,\psi)\right) z \\
&\quad + \mathcal{R}_1^{(n)}(\rho_1,\phi,\epsilon_1,\psi), \\
\dot{\rho}_1 &= -\frac{1}{2}\rho_1\epsilon_1, \\
\dot{\epsilon}_1 &= 2\epsilon_1^2, \\
\dot{\phi} &= \epsilon_1\left(((1-\xi)\phi + s)\left(1 - \frac{\rho_1^2\epsilon_1^2}{1-\xi}F(\rho_1\epsilon_1^2)\right) + V^{(n)}(A(\psi)z,\rho_1,\phi,\rho_1\epsilon_1)\right),
\end{aligned} \tag{104}$$

and

$$\dot{\psi} = \rho_1^{-1}, \tag{105}$$

after division of the right-hand side by ρ_1. Here

$$T_1^{(n)} = -\frac{1}{2}\delta + \mathcal{O}(\rho_1+\epsilon_1), \quad \Omega_1^{(n)} = \mathcal{O}(\rho_1+\epsilon_1), \tag{106}$$

and

$$R_1^{(n)}(z,\rho_1,\phi,\epsilon_1,\psi) = \mathcal{O}(\rho_1^n), \quad \mathcal{R}_1^{(n)}(\rho_1,\phi,\epsilon_1,\psi) = \mathcal{O}(\rho_1^{n+2}\epsilon_1),\ V^{(n)} = \mathcal{O}(z+\rho_1^2). \tag{107}$$

The system (104) is still $\mathcal{S}_\nu$-symmetric; recall Lemma 22. We consider the set

$$W_1: \quad z \in [-\sigma,\sigma]^2,\ \rho_1 \in [0,\nu],\ \epsilon_1 \in [0,\nu],\ \phi_1 \in [-\varpi^{-1},-\varpi],\ \psi \in S^1,$$

after possibly decreasing $\sigma > 0$ slightly.

Notice that $\rho_1 = 0$ is singular in (105), but the right-hand sides of the (z,ϵ_1,ϕ)-equations are well-defined there; cf. (104), (106), and (107). In particular, any point $(z,\epsilon_1,\phi_1) = (0,0,\phi_1)$ is an equilibrium of this system and the linearization has eigenvalues $0, -\frac{1}{2}\delta$, both of algebraic multiplicity two. Therefore we have gained hyperbolicity, albeit with the ψ-equation (105) singular at $\rho_1 = 0$. This allows us to obtain the following.

Proposition 23. *Fix $k \in \mathbb{N}$ and suppose $n \geq 2$. Then for $\nu > 0$ sufficiently small the following holds: There exists an attracting locally invariant manifold $M_{a,1}$ of (104) within W_1 as the graph*

$$M_{a,1}: \quad z = \rho_1^n \epsilon_1 A(\psi)^T m_1(\rho_1, \phi, \epsilon_1) \tag{108}$$

with $m_1(\cdot,\cdot,\cdot)$ Lipshitz continuous and $A(\psi) \in SO(2)$ (see (95)). Also the first k partial derivatives with respect to ϕ,

$$\partial_{\phi^i} m_1(\rho_1, \phi, \epsilon_1) \quad \text{with } 1 \leq i \leq k,$$

exist and are Lipshitz continuous.

Proof. See Appendix C. ∎

Remark 24. In the proof of Proposition 23 in Appendix C, we actually blow up $\rho_1 = \epsilon_1 = 0$, $z = 0$ further by introducing

$$z = \rho_1^n \epsilon_1 z_1. \tag{109}$$

The dynamics of (z_1, ϵ_1, ϕ) is then well-defined for $\rho_1 = 0$. See (122). Recall that in (104) the ϕ-equation actually depends upon ψ for $\rho_1 = 0$. It is therefore tempting to include $z = \bar{\rho}^n \bar{z}$ in the blowup (98) (and apply a consecutive blowup of $\epsilon_1 = 0, z_1 = 0$ in the proof of Proposition 23 to finally obtain (109) in chart (99)). This approach might allow for improved estimates of $o(1)$ in Theorem 6, but we did not find an easy way to deal with the subsequent details in the chart (100).

The invariant manifold

$$M_{a,1}(\varepsilon) \equiv M_{a,1} \cap \{\rho_1^4 \epsilon_1 = \varepsilon\} \tag{110}$$

can be viewed as an extension of Fenichel's slow manifold $S_{a,\varepsilon}$ up until $\theta = -(\varepsilon\nu^{-1})^{1/2}$ with $\phi \in [-\varpi^{-1}(\varepsilon\nu^{-1})^{1/2}, -\varpi(\varepsilon\nu^{-1})^{1/2}]$ by setting $\epsilon_1 = \nu$ in (102), together with (99) and (43), for ν sufficiently small but fixed with respect to ε. Note that there is a uniform contraction along $M_{a,1}(\varepsilon)$. In terms of $(\tilde{y}_n, \tilde{w}_n)$, the invariant manifold $M_{a,1}$ becomes a graph over $(\rho_1, \phi_1, \epsilon_1)$,

$$(\tilde{y}_n, \tilde{w}_n) = \rho_1^n \epsilon_1 m_1(\rho_1, \phi, \epsilon_1)$$

(by (94) using $AA^T = I$), which is independent of ψ as desired.

From (104), the reduced problem on $M_{a,1}$ becomes

$$\begin{aligned}
\dot{\rho}_1 &= -\frac{1}{2}\rho_1, \\
\dot{\epsilon}_1 &= 2\epsilon_1, \\
\dot{\phi} &= ((1-\xi)\phi + s)\left(1 - \frac{\rho_1^2\epsilon_1^2}{1-\xi} F(\rho_1\epsilon_1^2)\right) + V^{(n)}(\rho_1^n \epsilon_1 m_1(\rho_1, \phi, \epsilon_1), \rho_1, \phi, \rho_1\epsilon_1),
\end{aligned}$$

after division of the right-hand side by ϵ_1. The reduced problem is also independent of ψ as desired. Notice that

$$p_1: \quad \phi = -\frac{s}{1-\xi},\ \rho_1 = 0, \epsilon_1 = 0,$$

is hyperbolic. The invariant line

$$\phi = -\frac{s}{1-\xi},\ \rho_1 = 0,\ \epsilon_1 \geq 0,$$

within $M_{a,1} \cap \{\rho_2 = 0\}$ corresponds to l_2, as given in (55). As in (76), it is a strong unstable manifold of p_1 within $\rho_2 = 0$. The 1D stable manifold, contained within $\{\epsilon_1 = 0\}$, corresponds to the singular strong canard in this chart.

Setting $\epsilon_1 = \nu$ gives $\rho_1 = (\varepsilon/\nu)^{1/4}$ by the conservation (102). Therefore

$$M_{a,1}(\varepsilon) \cap \{\epsilon_1 = \nu\}: \quad z = (\varepsilon/\nu)^{n/4}\, \nu A(\psi)^T m_1(\rho_1(\varepsilon), \phi, \nu) = A(\psi)^T \mathcal{O}(\varepsilon^{n/4}); \tag{111}$$

cf. (108). Henceforth we suppose that $n \geq 4$.

B.5. Chart (100). In this chart we obtain the following equations from (96):

$$\begin{aligned}
\dot{z} &= \left(\begin{pmatrix} T_2^{(n)}(|z|^2, r_2, \phi, \rho_2) & \Omega_2^{(n)}(|z|^2, r_2, \phi, \rho_2) \\ -\Omega_2^{(n)}(|z|^2, r_2, \phi, \rho_2) & T_2^{(n)}(|z|^2, r_2, \phi, \rho_2) \end{pmatrix} + R_2^{(n)}(z, r_2, \phi, \rho_1, \psi) \right) z \\
&\quad + \mathcal{R}_2^{(n)}(r_2, \phi, \rho_1, \psi), \\
\dot{r}_2 &= -2r_2, \\
\dot{\phi} &= ((1-\xi)\phi + s)\left(1 - \frac{\rho_2^2}{1-\xi} F(\rho_2^2)\right) + V^{(n)}(A(\psi)z, \rho_2 r_2, \phi, \rho_2), \\
\dot{\rho}_2 &= \frac{3}{2}\rho_2,
\end{aligned} \tag{112}$$

and

$$\dot{\psi} = \rho_2^{-1}, \tag{113}$$

after division of the right-hand side by ρ_2. Here

$$T_2^{(n)} = \frac{1}{2}\left(\frac{1}{2} + \xi\right) + \mathcal{O}(r_2 + \rho_2), \quad \Omega_2^{(n)} = \mathcal{O}(r_2 + \rho_2),$$

and

$$R_2^{(n)}(z, r_2, \phi, \rho_2, \psi) = \mathcal{O}(\rho_2^n), \quad \mathcal{R}_2^{(n)}(r_2, \phi, \rho_2, \psi) = \mathcal{O}(\rho_2^{n+2} r_2). \tag{114}$$

Also

$$V^{(n)}(A(\psi)z, \rho_2 r_2, \phi, \rho_2) = \mathcal{O}(A(\psi)z + r_2(\rho_2 + r_2)).$$

As above, we notice that $\rho_2 = 0$ is well-defined for the right-hand side of (112). But now $z = r_2 = 0$, $\phi = (1-\xi)^{-1}s$ is a hyperbolic equilibrium, the linearization having the real eigenvalues $\frac{1}{2}\left(\frac{1}{2}+\xi\right)$, -2, $(1-\xi)$.

Let

$$W_2: \quad z \in [-\sigma,\sigma]^2,\ \rho_2 \in [0,\nu],\ r_2 \in [0,\nu],\ \phi_1 \in [-\varpi^{-1},-\varpi],\ \psi \in S^1.$$

Proposition 25. *Fix any $\eta \in (0,1)$, $n \geq 4$, and let ν be sufficiently small. Then for $0 < \varepsilon \ll 1$ the forward flow of $M_{a,2}(\varepsilon)$ intersects the $\{\rho_2 = \nu\}$-face of the box W_2 in a C^1-graph:*

$$z = A(\psi)^T m_{2,\varepsilon}(\phi)$$

with

$$m_{2,\varepsilon}(\phi) = \mathcal{O}(\varepsilon^{\eta(7-2\xi)/24}) = \mathcal{O}(\varepsilon^{5/24}), \quad m'_{2,\varepsilon}(\phi) = \mathcal{O}(\varepsilon^{1/12}). \tag{115}$$

Proof. Consider (112) with $n \geq 4$. The manifold $M_{a,1}(\epsilon)$ from chart $\bar{\rho} = 1$ enters the chart $\bar{\epsilon} = 1$ (100) at $r_2 = \nu^{-1}$, cf. (101), as a graph (111). We then apply a finite time flow map to go from $r_2 = \nu^{-1}$ to the $\{r_2 = \nu\}$-face of the box W_2, with ν small, which we then use as new initial conditions. By (111) we then have $z(0) = A(\psi)^T\mathcal{O}(\varepsilon^{n/4})$; a C^1-graph over $(\phi,\psi) \in [-\varpi^{-1},-\varpi]\times S^1$. Subsequently we work in W_2 only and define an exit time T by the condition $\rho_2(T) = \nu$. Solving the ρ_2-equation we obtain

$$T = \ln(\varepsilon^{-1/6}\nu^{7/6}), \tag{116}$$

using $\rho_2(0) = \varepsilon^{1/4}\nu^{-3/4}$ by (103).

Let

$$\zeta = \frac{1}{2}\left(\frac{1}{2}+\xi\right).$$

Then from the z-equation we obtain

$$\left(e^{-\zeta t}|z(t)|\right) \leq |z(0)| + \int_0^t c_1\left(\nu\left(e^{-\zeta u}|z(u)|\right) + \varepsilon^{1/3}\right)du,$$

while $\phi \in [-\varpi^{-1},-\varpi]$, r_2, $\rho_2 \leq \nu$.

$$|\mathcal{R}_2^{(n)}| \leq c_1\varepsilon^{1/3}$$

for all $\varepsilon \ll 1$. This follows from (103) and (114). Then by Gronwall's inequality for every ν and ε sufficiently small we have that

$$\begin{aligned} |z(T)| &\leq e^{(\zeta+c_1\nu)T}|z(0)| + c_1 e^{(\zeta+c_2\nu)T}\varepsilon^{1/3} \\ &\leq c_3\varepsilon^{1/3-(\zeta/6+c_3\nu)} \leq c_4\varepsilon^{5/24}, \end{aligned} \tag{117}$$

using $n \geq 4$, where c_2, c_3, and $c_4(\xi)$ are sufficiently large. In the last equality we used the fact that $\zeta < \frac{3}{4}$ and taken ν sufficiently small. This proves the first estimate in (115).

For the second estimate, we consider the variational equations obtained by differentiating the (z, ϕ)-equations with respect to $\phi(0) = \phi_0$. This gives

$$\left(e^{-\zeta t}|\tilde{z}(t)|\right) \leq |\tilde{z}(0)| + \int_0^t c_5\nu \left(\left(e^{-\zeta u}|\tilde{z}(u)|\right) + \varepsilon^{1/3-(\zeta/6+c_3\nu)}e^{-\beta u}\left(e^{-(1-\xi)u}|\tilde{\phi}(u)|\right)\right) du,$$
$$\left(e^{-(1-\xi)t}|\tilde{\phi}(t)|\right) \leq 1 + \int_0^t c_5\nu \left(\left(e^{-(1-\xi)u}|\tilde{\phi}(u)|\right) + e^{\beta u}\left(e^{-\zeta u}|\tilde{z}(u)|\right)\right) du$$

for c_5 sufficiently large, where for simplicity we have set

$$\beta = \zeta - (1-\xi) = \frac{3}{4}(2\xi - 1)$$

and introduced the following notation:

$$\tilde{z}(t) = \frac{\partial z}{\partial \phi_0}(t), \quad \tilde{\phi}(t) = \frac{\partial \phi}{\partial \phi_0}(t).$$

Notice $\tilde{z}(0) = \mathcal{O}(\varepsilon^{(n-2)/4})$ and $\tilde{\phi}(0) = 1$. Then $m'_{2,\varepsilon}(\phi)$ in (115) becomes $\tilde{z}(T)\tilde{\phi}(T)^{-1}$ by the chain rule. Suppose first that $\xi \leq \frac{1}{2}$ so that $\beta \leq 0$. Then

$$\left(e^{-\zeta t}|\tilde{z}(t)|\right) \leq |\tilde{z}(0)| + \int_0^t c_6\nu \left(\left(e^{-\zeta u}|\tilde{z}(u)|\right) + \varepsilon^{(1+\xi)/6-c_2\nu}\left(e^{-(1-\xi)u}|\tilde{\phi}(u)|\right)\right) du, \tag{118}$$
$$\left(e^{-(1-\xi)t}|\tilde{\phi}(t)|\right) \leq 1 + \int_0^t c_6\nu \left(\left(e^{-(1-\xi)u}|\tilde{\phi}(u)|\right) + \left(e^{-\zeta u}|\tilde{z}(u)|\right)\right) du$$

for $t \in [0, T]$ with c_6 sufficiently large, using here that

$$\varepsilon^{1/3-(\zeta/6+c_2\nu)}e^{-\beta u} \leq \varepsilon^{1/3-(\zeta/6+c_2\nu)}e^{-\beta T} \leq c_6\varepsilon^{1/3-(\zeta-\beta)/6-c_2\nu} = c_6\varepsilon^{(1+\xi)/6-c_2\nu}$$

for every $u \in [0, T]$, and all ε sufficiently small. Therefore by Gronwall's inequality, the following estimate holds true for all ν sufficiently small,

$$|\tilde{z}(t)| + |\tilde{\phi}(t)| \leq c_7 e^{((1-\xi)+c_7\nu)t}, \tag{119}$$

taking c_7 sufficiently large and using that $(1-\xi) \geq \zeta$ given that $\beta \leq 0$ by assumption. But then by (118)

$$\left(e^{-\zeta t}|\tilde{z}(t)|\right) \leq |\tilde{z}(0)| + c_8\nu\left(\int_0^t \left(e^{-\zeta u}|\tilde{z}(u)|\right) du + \varepsilon^{(1+\xi)/6-c_8\nu}\right),$$

using (119) to estimate $e^{-(1-\xi)t}|\tilde{\phi}(t)| \leq c_7 e^{c_7\nu}$. For ν sufficiently small we therefore have by Gronwall's inequality that

$$|\tilde{z}(T)| \leq c_9 e^{(\zeta+c_9\nu)T}\varepsilon^{(1+\xi)/6-c_9\nu} \leq c_9\varepsilon^{1/8} \leq c_9\varepsilon^{1/12}$$

for all ε sufficiently small. Here we have used (116) and the fact that

$$(1+\xi)/6 - \zeta/6 > \frac{1}{8}.$$

Now, given $\tilde{z}(t)$ the equation for $\tilde{\phi}$ is a linear, scalar, and nonautonomous ODE. Solving this linear equation and using the estimate on $\tilde{z}$ it is then straightforward to estimate $|\tilde{\phi}(T)| \geq C_3\varepsilon^{-(1+\xi)/6+C_3^{-1}\nu} \geq C_3$ uniformly from below for $C_3 > 0$ and $\nu > 0$ sufficiently small and all $0 < \varepsilon \ll 1$. This allows us to estimate $m'_{2,\varepsilon}(\phi)$ for $\xi \leq \frac{1}{2}$ as follows:

$$|m'_{2,\varepsilon}(\phi)| \leq C_3^{-1}c_9\varepsilon^{1/8} \leq C_3^{-1}c_9\varepsilon^{1/12}.$$

Now suppose that $\xi > \frac{1}{2}$ so that $\beta > 0$. Then we scale $\tilde{z}$ as

$$\tilde{z}(t) = e^{-\beta T}\hat{z}(t),$$

introducing $\hat{z}(t)$. This gives

$$\begin{aligned}
\left(e^{-\zeta t}|\hat{z}(t)|\right) &\leq |\hat{z}(0)| + \int_0^t c_{10}\nu\left(\left(e^{-\zeta u}|\hat{z}(u)|\right) + \varepsilon^{1/3-(\zeta/6+c_2\nu)}e^{\beta(T-u)}\left(e^{-(1-\xi)u}|\tilde{\phi}(u)|\right)\right)du \\
&\leq |\hat{z}(0)| + \int_0^t c_{11}\nu\left(\left(e^{-\zeta u}|\hat{z}(u)|\right) + \varepsilon^{1/12-c_{12}\nu}\left(e^{-(1-\xi)u}|\tilde{\phi}(u)|\right)\right)du \\
\left(e^{-(1-\xi)t}|\tilde{\phi}(t)|\right) &\leq 1 + \int_0^t c_{10}\nu\left(\left(e^{-(1-\xi)u}|\tilde{\phi}(u)|\right) + e^{-\beta(T-u)}\left(e^{-\zeta u}|\hat{z}(u)|\right)\right)du \\
&\leq 1 + \int_0^t c_{10}\nu\left(\left(e^{-(1-\xi)u}|\tilde{\phi}(u)|\right) + \left(e^{-\zeta u}|\hat{z}(u)|\right)\right)du
\end{aligned}$$

for $t \in [0, T]$. Hence

$$|\hat{z}(t)| + |\tilde{\phi}(t)| \leq c_{13}e^{(\zeta+c_{14}\nu)t} \tag{120}$$

for ν sufficiently small. But then

$$\left(e^{-\zeta t}|\hat{z}(t)|\right) \leq |\hat{z}(0)| + c_{15}\nu\left(\int_0^t \left(e^{-\zeta u}|\hat{z}(u)|\right)du + \varepsilon^{1/3-(\zeta/6+c_{16}\nu)}e^{\beta T}\right),$$

since $e^{-(1-\xi)t}|\tilde{\phi}(t)| \leq c_{13}e^{c_{14}\nu t}$ by (120). Now we return to $\tilde{z}$ by multiplying through by $e^{-\beta T}$. This gives

$$\left(e^{-\zeta t}|\tilde{z}(t)|\right) \leq |\tilde{z}(0)| + c_{17}\nu\left(\int_0^t \left(e^{-\zeta u}|\tilde{z}(u)|\right)du + \varepsilon^{1/3-(\zeta/6+c_{18}\nu)}\right).$$

Then by Gronwall's inequality

$$|\tilde{z}(T)| \leq c_{19}e^{\zeta T+c_{17}\nu}\varepsilon^{1/3-(\zeta/6+c_{18}\nu)} \leq c_{20}\varepsilon^{1/12},$$

using (116) and

$$1/3 - \zeta/3 > \frac{1}{12}.$$

■

As above, we can easily estimate $|\tilde{\phi}(T)| \geq C_3$ uniformly from below. This completes the proof of the estimate for $m'_{2,\varepsilon}(\phi)$ in (115).

Proposition 25 implies Proposition 19 since $\epsilon_1 = \rho_2$. This therefore completes the proof.

Appendix C. Proof of Proposition 23.

Consider (104)–(107) and set $z = \rho_1^n \epsilon_1 z_1$ to get

$$
\begin{aligned}
\dot{z_1} &= -\frac{1}{2}\delta z_1 + \tilde{R}(z_1, \rho_1, \epsilon_1, \phi, \psi),\\
\dot{\rho}_1 &= -\frac{1}{2}\rho_1 \epsilon_1,\\
\dot{\epsilon}_1 &= 2\epsilon_1^2,\\
\dot{\phi} &= \epsilon_1((1-\xi)\phi + s) + \tilde{V}(A(\psi)z_1, \rho_1, \phi, \epsilon_1),\\
\dot{\psi} &= \rho_1^{-1},
\end{aligned}
\tag{121}
$$

where now, using $n \geq 2$,

$$
\begin{aligned}
\tilde{R}(z_1, \rho_1, \epsilon_1, \psi) &= \frac{1}{2}n\epsilon_1^2 z_1 - 2\epsilon_1 z_1 + \left(\begin{pmatrix} T_1^{(n)}(|z|^2, \rho_1, \phi, \epsilon_1) & \Omega_1^{(n)}(|z|^2, \rho_1, \phi, \epsilon_1) \\ -\Omega_1^{(n)}(|z|^2, \rho_1, \phi, \epsilon_1) & T_1^{(n)}(|z|^2, \rho_1, \phi, \epsilon_1) \end{pmatrix} \right.\\
&\quad \left. + \frac{1}{2}\delta I + R_1^{(n)}(z, \rho_1, \phi, \epsilon_1, \psi) \right) z_1 + \rho_1^{-n}\epsilon_1^{-1}\mathcal{R}_1^{(n)}(\rho_1, \phi, \epsilon_1, \psi)\\
&= \mathcal{O}(z_1(\epsilon_1 + \rho_1) + \rho_1^2),\\
\tilde{V}(A(\psi)z_1, \rho_1, \phi, \epsilon_1) &= \epsilon_1 \left(-((1-\xi)\phi + s)\frac{\rho_1^2\epsilon_1^2}{1-\xi}F(\rho_1\epsilon_1^2) + V^{(n)}(\rho_1^n\epsilon_1 A(\psi)z_1, \rho_1, \phi, \rho_1\epsilon_1) \right),\\
&= \mathcal{O}(\epsilon_1(\epsilon_1 + \rho_1))
\end{aligned}
$$

are both smooth functions. In particular, $\tilde{R}(z_1, 0, \epsilon_1, \psi)$ and $\tilde{V}(A(\psi)z_1, 0, \phi, \epsilon_1)$ are both independent of ψ.

By modifying the standard proof of the existence of a center manifold using the contraction mapping theorem, we can now prove the existence of a locally invariant manifold $M_{a,1}$. We provide all of the details below. It will be useful to introduce ω and $\hat{\omega}$ as $\omega = (\hat{\omega}, \phi)$, where $\hat{\omega} = (\rho_1, \epsilon_1)$. Furthermore, let $\Psi : \mathbb{R} \to [0,1]$ be a C^∞ cut-off function satisfying $\Psi(-x) = \Psi(x)$, $\Psi(x) = 1$ for all $x \in [0,1]$, and $\Psi(x) = 0$ for all $x \geq 2$. Similarly, we let $\Phi : \mathbb{R} \to [0,1]$ be a C^∞ function satisfying

$$
\Phi|_{[-\varpi^{-1}, -\varpi]} = 1, \quad \Phi|_{(-\infty, -2\varpi^{-1}) \cup (-\varpi^{-1}/2, \infty)} = 0.
$$

Let $\sigma > 0$. We then consider the following modified system:

$$
\begin{aligned}
\dot{z_1} &= -\frac{1}{2}\delta z_1 + \tilde{R}(z_1, \omega, \psi),\\
\dot{\rho}_1 &= -\frac{1}{2}\Psi\left(\frac{|\hat{\omega}|}{\sigma}\right)\rho_1\epsilon_1,\\
\dot{\epsilon}_1 &= 2\Psi\left(\frac{|\hat{\omega}|}{\sigma}\right)\epsilon_1^2,\\
\dot{\phi} &= \tilde{P}(z_1, \omega, \psi),\\
\dot{\psi} &= \rho_1^{-1},
\end{aligned}
\tag{122}
$$

where

$$\tilde{R}(z_1,\omega,\psi) = \Psi\left(\frac{|\hat{\omega}|}{\sigma}\right)\Phi(\phi)\,R(z_1,\omega,\psi),$$

$$\tilde{P}(z_1,\omega,\psi) = \Psi\left(\frac{|\hat{\omega}|}{\sigma}\right)\Phi(\phi)\left(\epsilon_1((1-\xi)\phi+s)+\tilde{V}(A(\psi)z_1,\omega)\right).$$

Also $\tilde{R}$ and $\tilde{P}$ are $\mathcal{S}_\nu$-equivariant and $\mathcal{S}_\nu$-invariant, respectively; recall (97). Let $B_r(\hat{\omega}_0) = \{\hat{\omega}\in\mathbb{R}^2 | |\hat{\omega}-\hat{\omega}_0| < r\}$ denote the open desk centered at $\hat{\omega}_0$ with radius r. Then notice that (a) (122) coincides with (121) within $|\hat{\omega}|\le\sigma$, $\phi\in[-\varpi^{-1},-\varpi]$ (cf. the definition of Ψ and Φ) and (b) $\hat{\omega}_0\in B_{2\sigma}(0)$ implies that $\hat{\omega}(t)\in B_{2\sigma}(0)$ for all t. We therefore consider the following set:

$$\mathcal{W} = \{\omega=(\hat{\omega},\phi)\in\overline{B_{2\sigma}(0)}\times\mathbb{R}\}.$$

Lemma 26. *There exists a constant $C_1>0$ so that the following estimates hold:*

$$|\tilde{R}(z_1',\omega',\psi)-\tilde{R}(z_1,\omega,\psi)| \le C_1\sigma\left(|\omega'-w|+|z_1'-z_1|\right),$$

$$|\tilde{P}(z_1',\omega',\psi)-\tilde{P}(z_1,\omega,\psi)| \le C_1\left(|\epsilon_1'-\epsilon_1|+\sigma\left(|\phi'-\phi|+|\rho_1'-\rho_1|+|z_1'-z_1|\right)\right),$$

and

$$|\tilde{R}(z_1,\omega,\psi)| \le C_1\sigma^2$$

for all $\omega'=(\rho_1',\epsilon_1',\phi'),\omega=(\rho_1,\epsilon_1,\phi)\in\mathcal{W}$, $|z_1|$, $|z_1'|\le\sigma$, and $\psi\in S^1$.

Proof. The proof is straightforward. ∎

For $p_0>0$ and $p_1>0$ we then define $\mathcal{X}(p_0,p_1)$ as the set of Lipschitz functions $h:\mathcal{W}\times S^1\to\mathbb{R}^2$ satisfying

$$h(0,\psi)=0,\quad |h(\omega,\psi)|\le p_0,\quad |h(\omega+\upsilon,\psi)-h(\omega,\psi)|\le p_1|\upsilon|\quad\forall\,\omega,\omega+\upsilon\in\mathcal{W}.$$

With the supremum norm

$$\|h\| = \sup_{(\omega,\psi)\in\mathcal{W}\times S^1}|h(\omega,\psi)|,$$

$\mathcal{X}(p_0,p_1)$ is complete.

For $h\in\mathcal{X}(p_0,p_1)$ and $\omega_0=(\rho_{10},\epsilon_{10},\phi_{10})\in\mathcal{W}$ with $\rho_{10}\neq0$, we let

$$(\omega(t,\omega_0,\psi_0,h),\ \psi(t,\omega_0,\psi_0,h))$$

be the solution of

$$\dot{\rho}_1 = -\frac{1}{2}\Psi\left(\frac{|\hat{\omega}|}{\sigma}\right)\rho_1\epsilon_1,$$

$$\dot{\epsilon}_1 = 2\Psi\left(\frac{|\hat{\omega}|}{\sigma}\right)\epsilon_1^2,$$

$$\dot{\phi} = \tilde{P}(h,\omega,\psi) = \Psi\left(\frac{|\hat{\omega}|}{\sigma}\right)\Phi(\phi)\left(\epsilon_1((1-\xi)\phi+s)+\tilde{V}(A(\psi)h(w),\omega)\right),$$

$$\dot{\psi} = \rho_1^{-1},$$

satisfying

$$(\omega(0,\omega_0,\psi_0,h),\ \psi(0,\omega_0,\psi_0,h)) = (\omega_0,\ \psi_0)\,.$$

For $\rho_{10} = 0$ we define $\omega(t,\omega_0,\psi_0,h)$ similarly. Here it is (cf. (121)) simply independent of ψ_0. Finally, we set $\psi(t,\omega_0,\psi_0,h) = \psi_0$ when $\rho_{10} = 0$ for all t. This particular choice is not important.

Lemma 27. *Let $\omega' = (\rho_1',\epsilon_1',\phi') = \omega(t,\omega_0',\psi_0,h)$ and $\omega = (\rho_1,\epsilon_1,\phi) = \omega(t,\omega_0,\psi_0,h)$ with $h \in \mathcal{X}(p_0,p_1)$ and $\omega_0' = (\rho_{10}',\epsilon_{10}',\phi_0'),\omega_0 = (\rho_{10},\epsilon_{10},\phi_0) \in \mathcal{W}$. Then there exists a constant $C_2 > 0$ so that the following estimates hold:*

$$\begin{aligned}
|\epsilon_1' - \epsilon_1| &\le e^{-C_2\sigma t}|\epsilon_{10}' - \epsilon_{10}|,\\
|\rho_1' - \rho_1| &\le C_2 e^{-C_2\sigma t}\left(|\rho_{10}' - \rho_{10}| + |\epsilon_{10}' - \epsilon_{10}|\right),\\
|\phi' - \phi| &\le C_2(-t)e^{-C_2\sigma t}\left(|\rho_{10}' - \rho_{10}| + |\epsilon_{10}' - \epsilon_{10}| + |\phi_0' - \phi_0|\right)
\end{aligned}$$

for $t \le 0$.

Proof. From the ϵ_1-equation we directly obtain

$$|\epsilon_1'(t) - \epsilon_1(t)| \le |\epsilon_{10}' - \epsilon_{10}| + \int_t^0 c_1\sigma|\epsilon_1'(\tau) - \epsilon(\tau)|d\tau$$

for $c_1 > 0$ sufficiently large, and therefore by Gronwall's inequality

$$|\epsilon_1' - \epsilon_1| \le e^{-c_1\sigma t}|\epsilon_{10}' - \epsilon_{10}|, \quad t \le 0.$$

But then from the ρ_1-equation

$$\begin{aligned}
|\rho_1' - \rho_1| &\le |\rho_{10}' - \rho_{10}| + c_2\sigma\int_t^0 \left(|\epsilon_1'(\tau) - \epsilon_1(\tau)| + |\rho_1'(\tau) - \rho_1(\tau)|\right)d\tau\\
&\le |\rho_{10}' - \rho_{10}| + c_3 e^{-c_1\sigma t}|\epsilon_{10}' - \epsilon_{10}| + c_2\sigma\int_t^0 |\rho_1'(\tau) - \rho_1(\tau)|d\tau
\end{aligned}$$

for $c_3 > c_2 > 0$ sufficiently large. Then by Gronwall's inequality

$$|\rho_1' - \rho_1| \le c_3 e^{-c_4\sigma t}\left(|\rho_{10}' - \rho_{10}| + |\epsilon_{10}' - \epsilon_{10}|\right)$$

for $c_4 > 0$ sufficiently large. Finally, from the ϕ-equation,

$$\begin{aligned}
|\phi'(t) - \phi(t)| &\le |\phi_0' - \phi_0| + c_5\int_t^0 \left(|\epsilon_1'(\tau) - \epsilon_1(\tau)| + \sigma\big(|\phi'(\tau) - \phi(\tau)|\right.\\
&\quad \left. + |\rho_1'(\tau) - \rho_1(\tau)|\big)\right)d\tau\\
&\le |\phi_0' - \phi_0| + c_6(-t)e^{-c_7\sigma t}\left(|\epsilon_{10}' - \epsilon_{10}| + |\rho_{10}' - \rho_{10}|\right)\\
&\quad + c_5\sigma\int_t^0 |\phi'(\tau) - \phi(\tau)|d\tau,
\end{aligned}$$

using Lemma 26 and that $h \in \mathcal{X}(p_0,p_1)$. Therefore

$$|\phi'(t) - \phi(t)| \le c_8(-t)e^{-c_9\sigma t}\left(|\epsilon_{10}' - \epsilon_{10}| + |\rho_{10}' - \rho_{10}| + |\phi_0' - \phi_0|\right)$$

for $c_8 > 0$ and $c_9 > 0$ sufficiently large. This gives the desired result. ∎

Lemma 28. *Let* $\omega' = (\rho_1', \epsilon_1', \phi') \equiv \omega(t, \omega_0, \psi_0, h')$ *and* $\omega = (\rho_1, \epsilon_1, \phi) = \omega(t, \omega_0, \psi_0, h)$ *with* $h', h \in \mathcal{X}(p_0, p_1)$, *and* $\omega_0 = (\rho_{10}, \epsilon_{10}, \phi_0) \in \mathcal{W}$. *Then* $\epsilon_1' = \epsilon_1$, $\rho_1' = \rho_1$, *and there exists a constant* $C_3 > 0$ *so that the following estimate holds:*

$$|\phi' - \phi| \le C_3 \sigma(-t) e^{-C_3 \sigma t} \|h' - h\|,$$

for $t \le 0$.

Proof. The ϵ_1- and ρ_1-equations are independent of h. Therefore by the ϕ-equation

$$|\phi'(t) - \phi(t)| \le c_1 \sigma \int_t^0 \left(|\phi'(\tau) - \phi(\tau)| + \|h' - h\| \right) d\tau,$$

using Lemma 26, and then by Gronwall's inequality

$$|\phi' - \phi| \le c_1 \sigma(-t) e^{-c_1 \sigma t} \|h' - h\|.$$

■

Finally, we define $\mathcal{T} : \mathcal{X}(p_0, p_1) \to \mathcal{X}(p_0, p_1)$ as

$$(\mathcal{T}h)(\omega_0, \psi_0) = \int_{-\infty}^0 e^{\frac{1}{2}\delta t} \tilde{R}(h(\omega, \psi), \omega, \psi) dt,$$

where for simplicity

$$\omega = \omega(t, \omega_0, \psi_0, h), \quad \psi = \psi(t, \omega_0, \psi_0, h).$$

Proposition 29. *For* p_0 *and* σ *sufficiently small,* $\mathcal{T}$ *is a contraction on* $\mathcal{X}(p_0, p_1)$.

Proof. We set

$$p_0 = \sigma.$$

Then we show that $\mathcal{T} : \mathcal{X}(p_0, p_1) \to \mathcal{X}(p_0, p_1)$ is well-defined. Using Lemma 26, we obtain

$$|(\mathcal{T}h)(\omega_0, \psi_0)| \le c_1 \sigma^2$$

for any $\sigma > 0$ with $c_1 > 0$ sufficiently large. Thus $|(\mathcal{T}h)(\omega_0, \psi_0)| \le p_0 = \sigma$ for σ sufficiently small. Next, we have

$$|(\mathcal{T}h)(\omega_0', \psi_0) - (\mathcal{T}h)(\omega_0, \psi_0)| \le \int_{-\infty}^0 e^{\frac{1}{2}\delta t} C_1 (1 + p_1) \sigma |\omega'(t) - \omega(t)| dt,$$

using Lemma 26. Therefore by Lemma 27

$$\begin{aligned} |(\mathcal{T}h)(\omega_0', \psi_0) - (\mathcal{T}h)(\omega_0, \psi_0)| &\le C_1 (1 + p_1) \sigma \int_{-\infty}^0 (-t) e^{\frac{1}{2}\delta t - C_2 \sigma t} dt |\omega_0' - \omega_0| \\ &\le c_2 (1 + p_1) \sigma |\omega_0' - \omega_0| \end{aligned}$$

with $c_2 > 0$, for all σ sufficiently small. Therefore $\mathcal{T}$ is well-defined. Finally,

$$|(\mathcal{T}h')(\omega_0,\psi_0) - (\mathcal{T}h)(\omega_0,\psi_0)| \leq C_1\sigma \int_{-\infty}^{0} e^{\frac{1}{2}\delta t} \left(|\phi'(t) - \phi(t)| + \|h' - h\|\right) dt$$
$$\leq c_3\sigma \int_{-\infty}^{0} (-t) e^{\frac{1}{2}\delta t - C_3\sigma t} dt \|h' - h\| \leq c_4\sigma\|h' - h\|,$$

by Lemma 28, for c_4, $c_3 > 0$ sufficiently large, and all σ sufficiently small. The result then follows. ∎

The contraction mapping theorem guarantees the existence of a unique fixed point $h_* \in \mathcal{X}(p_0, p_1)$ of $\mathcal{T}$. The graph of h_* is our center manifold. The function h_* is C^k-smooth in ϕ. The key observation here is that ψ only depends upon $\hat{\omega}$; it is independent of ϕ. The result is therefore standard, following almost identical arguments to those used above. We skip the details. The smoothness in ρ_1, ϵ_1 is more delicate, but we do not need it for our purposes.

The following lemma completes the proof of Proposition 23.

Lemma 30. *The fixed point $h_*(\omega,\psi)$ of $\mathcal{T}$ on $\mathcal{X}(p_0,p_1)$ satisfies*

$$h_*(\omega,\psi) = A(\psi)^T m_1(\omega).$$

Proof. The modified system (122) is $\mathcal{S}_\nu$-equivariant; recall Lemma 22. This implies, by the uniqueness of h_*, that

$$z_1 = A(\nu)^T h_*(\omega, \psi - \nu) = h_*(\omega,\psi)$$

for all $\nu \in S^1$. Setting $\nu = \psi$ and $m_1(\omega) = h_*(\omega, 0)$ gives the desired result. ∎

REFERENCES

[1] E. Benoît, J. L. Callot, F. Diener, and M. Diener, *Chasse au canard*, Collect. Math., 31-32 (1981), pp. 37–119.

[2] A. Blumenthals, B. Brogliato, and F. Bertails-Descoubes, *The contact problem in Lagrangian systems subject to bilateral and unilateral constraints, with or without sliding Coulomb's friction: A tutorial*, Multibody Syst. Dyn., 38 (2016), pp. 43–76.

[3] R. Brach, *Impacts coefficients and tangential impacts*, J. Appl. Mech., 64 (1997), pp. 1014–1016.

[4] B. Brogliato, *Nonsmooth Mechanics*, 2nd ed., Springer, Berlin, 1999.

[5] M. Brøns, *Canard explosion of limit cycles in templator models of self-replication mechanisms*, J. Chem. Phys., 134 (2011).

[6] A. Champneys and P. Várkonyi, *The Painlevé paradox in contact mechanics*, IMA J. Appl. Math., 81 (2016), pp. 538–588.

[7] H. Chiba, *Periodic orbits and chaos in fast-slow systems with Bogdanov–Takens type fold points*, J. Differential Equations, 250 (2011), pp. 112–160, https://doi.org/10.1016/j.jde.2010.09.022.

[8] G. Darboux, *Étude géometrique sur les percussions et le choc des corps*, Bull. Sci. Math. Astron., 2e Ser., 4 (1880), pp. 126–160.

[9] M. Desroches and M. R. Jeffrey, *Canards and curvature: Nonsmooth approximation by pinching*, Nonlinearity, 24 (2011), pp. 1655–1682, https://doi.org/10.1088/0951-7715/24/5/014.

[10] M. di Bernardo, C. J. Budd, A. R. Champneys, and P. Kowalczyk, *Piecewise-Smooth Dynamical Systems: Theory and Applications*, Springer, Berlin, 2008.

[11] F. Dumortier, *Local study of planar vector fields: Singularities and their unfoldings*, in Structures in Dynamics: Finite Dimensional Deterministic Studies, Vol. 2, H. W. B. et al., eds., Springer, Berlin, 1991, pp. 161–241.
[12] F. Dumortier, *Techniques in the theory of local bifurcations: Blow-up, normal forms, nilpotent bifurcations, singular perturbations*, in Bifurcations and Periodic Orbits of Vector Fields, D. Schlomiuk, ed., NATO ASI Ser. 408, Springer, Berlin, 1993, pp. 19–73, https://doi.org/10.1007/978-94-015-8238-4_2.
[13] F. Dumortier and R. Roussarie, *Canard cycles and center manifolds*, Mem. Amer. Math. Soc., 121 (1996), pp. 1–96.
[14] P. E. Dupont and S. P. Yamajako, *Stability of frictional contact in constrained rigid-body dynamics*, IEEE Trans. Robot. Autom., 13 (1997), pp. 230–236.
[15] N. Fenichel, *Persistence and smoothness of invariant manifolds for flows*, Indiana Univ. Math. J., 21 (1971), pp. 193–226.
[16] N. Fenichel, *Asymptotic stability with rate conditions*, Indiana Univ. Math. J., 23 (1974), pp. 1109–1137.
[17] N. Fenichel, *Geometric singular perturbation theory for ordinary differential equations*, J. Differential Equations, 31 (1979), pp. 53–98.
[18] A. Filippov, *Differential Equations with Discontinuous Righthand Sides*, Math. Appl., Kluwer Academic Publishers, Norwell, MA, 1988.
[19] F. Génot and B. Brogliato, *New results on Painlevé paradoxes*, Eur. J. Mech. A Solids, 18 (1999), pp. 653–677.
[20] M. Haragus and G. Iooss, *Local Bifurcations, Center Manifolds, and Normal Forms in Infinite-Dimensional Dynamical Systems*, Springer, Berlin, 2011.
[21] S. J. Hogan and K. U. Kristiansen, *On the regularization of impact without collision: The Painlevé paradox and compliance*, Proc. Roy. Soc. Lond. A., 473 (2017), 20160773.
[22] A. Ivanov, *On the correctness of the basic problem of dynamics in systems with friction*, Prikl. Mat. Mekh., 50 (1986), pp. 547–550.
[23] C. Jones, *Geometric singular perturbation theory*, Lecture Notes in Math., Dynamical Systems (Montecatini Terme), Springer, Berlin, 1995.
[24] J. B. Keller, *Impact with friction*, J. Appl. Mech., 53 (1986), pp. 1–4.
[25] K. U. Kristiansen and S. J. Hogan, *On the use of blowup to study regularizations of singularities of piecewise smooth dynamical systems in* $\mathbb{R}^3$, SIAM J. Appl. Dyn. Syst., 14 (2015), pp. 382–422, https://doi.org/10.1137/140980995.
[26] K. U. Kristiansen and S. J. Hogan, *Regularizations of two-fold bifurcations in planar piecewise smooth systems using blowup*, SIAM J. Appl. Dyn. Syst., 14 (2015), pp. 1731–1786.
[27] K. U. Kristiansen and S. J. Hogan, *Resolution of the piecewise smooth visible-invisible two-fold singularity in* $\mathbb{R}^3$ *using regularization and blowup*, submitted, arXiv:1602.01026v5.
[28] M. Krupa and P. Szmolyan, *Extending geometric singular perturbation theory to nonhyperbolic points—Fold and canard points in two dimensions*, SIAM J. Math. Anal., 33 (2001), pp. 286–314.
[29] M. Krupa and P. Szmolyan, *Extending slow manifolds near transcritical and pitchfork singularities*, Nonlinearity, 14 (2001), 1473.
[30] M. Krupa and P. Szmolyan, *Relaxation oscillation and canard explosion*, J. Differential Equations, 174 (2001), pp. 312–368.
[31] C. Kuehn, *Multiple Time Scale Dynamics*, Springer, Berlin, 2015.
[32] J. S. Langer, *Theory of spinodal decomposition in alloys*, Ann. Phys., 65 (1971), pp. 53–86.
[33] R. E. Langer, *On the asymptotic forms of the solutions of ordinary linear differential equations of the third order in a region containing a turning point*, Trans. Amer. Math. Soc., 80 (1955), pp. 93–123.
[34] R. E. Langer, *The solutions of the differential equation* $v''' + \lambda^2 zv' + 3\mu\lambda^2 v = 0$, Duke Math. J., 22 (1955), pp. 525–541.
[35] L. Lecornu, *Sur la loi de Coulomb*, C. R. Séances Acad. Sci., 140 (1905), pp. 847–848.
[36] R. Leine, B. Brogliato, and H. Nijmeijer, *Periodic motion and bifurcations induced by the Painlevé paradox*, Eur. J. Mech. A Solids, 21 (2002), pp. 869–896.
[37] C. Liu, Z. Zhao, and B. Chen, *The bouncing motion appearing in a robotic system with unilateral constraint*, Nonlinear Dynam., 49 (2007), pp. 217–232.
[38] N. H. McClamroch, *A singular perturbation approach to modeling and control of manipulators constrained by a stiff environment*, in Proceedngs of the 28th Conference Decision Control, 1989, pp. 2407–2411.

[39] Y. I. Neimark and N. A. Fufayev, *The Painlevé paradoxes and the dynamics of a brake shoe*, J. Appl. Math. Mech., 59 (1995), pp. 343–352.
[40] Y. I. Neimark and V. N. Smirnova, *Singularly perturbed problems and the Painlevé problem*, Differ. Equ., 36 (2000), pp. 1639–1646.
[41] Y. I. Neimark and V. N. Smirnova, *Contrast structures, limit dynamics and the Painlevé paradox*, Differ. Equ., 37 (2001), pp. 1580–1588.
[42] A. Nordmark, P. Várkonyi, and A. Champneys, *Dynamics Beyond Dynamic Jam; Unfolding the Painlevé Paradox Singularity*, preprint, arXiv:1707.08343, 2016.
[43] Y. Or, *Painlevé's paradox and dynamic jamming in simple models of passive dynamic walking*, Regul. Chaotic Dyn., 19 (2014), pp. 64–80.
[44] Y. Or and E. Rimon, *Investigation of Painlevé's paradox and dynamic jamming during mechanism sliding motion*, Nonlinear Dynam., 67 (2012), pp. 1647–1668.
[45] P. Painlevé, *Sur les loi du frottement de glissement*, C. R. Séances Acad. Sci., 121 (1895), pp. 112–115.
[46] P. Painlevé, *Sur les loi du frottement de glissement*, C. R. Séances Acad. Sci., 141 (1905), pp. 401–405.
[47] P. Painlevé, *Sur les loi du frottement de glissement*, C. R. Séances Acad. Sci., 141 (1905), pp. 546–552.
[48] L. Perko, *Differential Equations and Dynamical Systems*, 3rd ed., Texts Appl. Math. 7, Springer, Berlin, 2001.
[49] P. Song, P. Kraus, V. Kumar, and P. E. Dupont, *Analysis of rigid-body dynamic models for simulation of systems with frictional contacts*, J. Appl. Mech., 68 (2001), pp. 118–128.
[50] D. E. Stewart, *Rigid-body dynamics with friction and impact*, SIAM Rev., 42 (2000), pp. 3–39.
[51] W. J. Stronge, *Energetically consistent calculations for oblique impact in unbalanced systems with friction*, J. Appl. Mech., 82 (2015), 081003.
[52] P. Szmolyan and M. Wechselberger, *Canards in* $\mathbb{R}^3$, J. Differential Equations, 177 (2001), pp. 419–453, https://doi.org/10.1006/jdeq.2001.4001.
[53] O. Vallée, *On the linear third order differential equation*, Lecture Notes in Phys. 518, 1999, pp. 340–347.
[54] O. Vallée and M. Soares, *Airy Functions and Applications to Physics*, World Scientific, River Edge, NJ, 2004.
[55] M. Wechselberger, *Existence and bifurcation of canards in* $\mathbb{R}^3$ *in the case of a folded node*, SIAM J. Appl. Dyn. Syst., 4 (2005), pp. 101–139, https://doi.org/10.1137/030601995.
[56] E. V. Wilms and H. Cohen, *Planar motion of a rigid body with a friction rotor*, J. Appl. Mech., 48 (1981), pp. 205–206.
[57] E. V. Wilms and H. Cohen, *The occurrence of Painlevé's paradox in the motion of a rotating shaft*, J. Appl. Mech., 64 (1997), pp. 1008–1010.
[58] Z. Zhao, C. Liu, B. Chen, and B. Brogliato, *Asymptotic analysis and Painlevé's paradox*, Multibody Syst. Dyn., 35 (2015), pp. 299–319.
[59] Z. Zhao, C. Liu, W. Ma, and B. Chen, *Experimental investigation of the Painlevé paradox in a robotic system*, J. Appl. Mech., 75 (2008), 041006.